Land use types affect soil microbial NO_3^- immobilization through changed fungal and bacterial contribution in alkaline soils of a subtropical montane agricultural landscape

Xingling Wang[1,2], Minghua Zhou[1*], Bo Zhu[1], Nicolas Brüggemann[3], Wei Zhang[4], Klaus Butterbach-Bahl[5,6]

[1] Key Laboratory of Mountain Surface Processes and Ecological Regulation, Institute of Mountain Hazards and Environment, Chinese Academy of Sciences, Chengdu 610041, PR China

[2] University of Chinese Academy of Sciences, Beijing 100049, PR China

[3] Institute of Bio- and Geosciences - Agrosphere (IBG-3), Forschungszentrum Jülich GmbH, 52425 Jülich, Germany

[4] Institute of Applied Ecology, Chinese Academy of Sciences, Shenyang 110016, PR China

[5] Pioneer Center Land-CRAFT, Department of Agroecology, Aarhus University, Aarhus C, 8000, Denmark

[6] Institute for Meteorology and Climate Research, Atmospheric Environmental Research, Karlsruhe Institute of Technology, D-82467 Garmisch-Partenkirchen, Germany

Corresponding author: Minghua Zhou E-mail: mhuazhou@imde.ac.cn

Abstract

Soil microbial nitrate (NO_3^-) immobilization plays a vital role in enhancing the nitrogen (N) retention in the subtropical montane agricultural landscapes. However, how and why the potential microbial NO_3^- immobilization and the relative contribution of fungi and bacteria vary across different land use types remain still unclear in the subtropical mosaic montane agricultural landscapes. Thus, in the present study, soil gross microbial NO_3^- immobilization rates as well as the respective contribution of fungi and bacteria were determined throughout the whole soil profiles for three land use types (woodland, orchard, and cropland) by using the ^{15}N tracing and amino sugar-based stable isotope probing (Amino sugars-SIP) techniques. The soil gross microbial NO_3^- immobilization rates in woodland soils were significantly higher than those in cropland and orchard soils across different soil layers ($p < 0.05$), and those of topsoil were significantly higher than those for subsoils (e.g., 20-40 cm) across different land use types ($p < 0.05$). Soil microbial biomass C (MBC) and N (MBN), organic C (SOC), total N (TN) and dissolved organic C (DOC) contents and C/N ratios were closely associated to gross microbial NO_3^- immobilization rates. Fungi played a greater role than bacteria in immobilizing soil NO_3^- in woodland and orchard soils but the opposite occurred in cropland soils that over 85% of the variations in fungal and bacterial NO_3^- immobilization rates could be explained by their respective phospholipid fatty acid-derived (PLFA-derived) biomass. The present study indicated that afforestation may be effective to enhance soil NO_3^- retention in alkaline soils, thereby likely decreasing the risk of NO_3^- losses in subtropical mosaic montane agricultural landscapes through enhancing the soil NO_3^- immobilization by both fungi and bacteria.

Keywords: Soil microbial NO_3^- immobilization; ^{15}N tracing technique; Amino sugars-SIP; Alkaline soils; Land use; Subtropical mosaic montane agricultural landscape

Introduction

In recent decades, the global nitrogen (N) cycle has increasingly become perturbed due to the overuse of N fertilizers in agriculture (Vitousek et al. 1997), and the associated N losses have resulted in serious environmental problems (Cui et al. 2013; Sebilo et al. 2013; Zhou et al. 2014). Soil NO_3^- leaching is a key environmental problem in agricultural landscapes worldwide as it can cause the eutrophication of surface water and the degradation of drinking water quality (Huygens et al. 2008; Zhou et al. 2016; Bijay-Singh and Craswell 2021). Thus, improving the understanding of mechanisms of soil NO_3^- retention and their key regulators is critical for mitigating NO_3^- leaching losses, alleviating negative environmental impacts and sustaining soil fertility (Zogg et al. 2000; Tahovská et al. 2013). Soil microbial NO_3^- immobilization has been suggested as an efficient way to improve soil NO_3^- retention (Stark and Hart 1997; Zogg et al. 2000; Booth et al. 2005; Li et al. 2019, 2020), but the mechanisms are poorly understood.

Soil microbial NO_3^- immobilization is controlled by soil biotic and abiotic properties, such as soil microbial biomass, the availabilities of C and N and clay contents (Zhang et al. 2013b; Wang et al. 2015; Nelson et al. 2016; Li et al. 2019; Zhang et al. 2022). The land use changes can alter those soil properties (Chang et al. 2012), which in turn affect soil microbial NO_3^- immobilization. Soil fungi and bacteria are the two dominant microorganisms to immobilize NO_3^- (Marzluf 1997; Myrold and Posavatz 2007; Boyle et al. 2008; Li et al. 2019, 2020). Thus some studies suggested that the effects of land use change on soil microbial NO_3^- immobilization could be likely to be associated with the changes in soil fungal and bacterial biomass and their respective capacity of assimilating NO_3^- in soils (de Vries and Bardgett 2012; Manoharan et al. 2017). Li et al. (2019) found that soil microbial NO_3^- immobilization decreased following the conversion of woodland to agricultural land, as the result of decreased fungal and bacterial NO_3^- immobilization, and this was closely correlated with the quantity and quality of soil organic C. In addition, land use changes affect soil pH, which influences soil microbial NO_3^- immobilization especially the activity of fungi (Rice and Tiedje 1989; Shi and Norton 2000; Zhang et al. 2013a, b; Wang et al. 2015; Li et al. 2019). It is noteworthy that soil pH may exert overwhelming impact on the size, activity and community structure of soil microbes (Jones et al. 2019) Additionally, the responses of bacterial and fugal communities towards soil pH are prominently different, and the bacterial community is even more sensitive to soil pH than the fungal community in agricultural soils (Rousk et al. 2010). These findings raise the intriguing possibility that soil pH ultimately affect microbial NO_3^- immobilization. Up to date, most of the available studies focused on acidic soils (e.g., Banning et al. 2008; Zhang et al. 2013b; Allen et al. 2015; Vázquez et al. 2019; Yokobe et al. 2020), while few studies considered microbial NO_3^-immobilization in alkaline soils, especially those of the subtropical montane agricultural landscapes that are often identified as hotspots of hydrological NO_3^- loss (Zhou et al. 2012). Therefore, the knowledge gap that quantify soil microbial NO_3^- immobilization and distinguish the respective role of fungi and bacteria as well as the underlying mechanisms as affected by land use types in alkaline soils limit the unraveling of soil N retention mechanisms for mitigating N losses.

There are inconsistent results on the relative importance of fungi and bacteria in immobilizing NO_3^- in soils, likely due to their divergences in physiology, morphology, lifestyles and quantities in soils (Six et al. 2006; Rousk and Bååth 2007; Lauber et al. 2008; Bottomley et al. 2012). Some studies showed that fungi played a significant role in assimilating NO_3^- in soil (Marzluf 1997; Cheshire et al. 1999; de Vries et al. 2011), while other studies showed that the potential NO_3^- immobilization by bacteria was comparable to or even greater than that by fungi (Myrold and Posavatz 2007; Boyle et al. 2008). Despite the fact that both fungi and bacteria can conserve NO_3^- in soils, the number of reports on the relative contribution of fungi and bacteria is limited, most likely caused by methodological limitations for quantifying the respective fungal and bacterial NO_3^- immobilization (Booth et al. 2005; Myrold and Posavatz 2007; Boyle et al. 2008). Recently, the amino sugars-based stable isotope probing (Amino sugars-SIP) method has been developed and applied to differentiate the soil NO_3^- immobilization process between fungi and bacteria (Li et al. 2019, 2020). The amino sugars are stable N pools with mean residence time of 2–8 years (Derrien and Amelung 2011; Glaser et al. 2006) and reliable microbial residue biomarkers due to their different microbial origins in soils (Amelung 2001; Zhang and Amelung 1996). Muramic acid (Mur) originates exclusively from bacterial peptidoglycan (Parsons 1981; Amelung 2001), whereas glucosamine (GluN) is primarily from fungal cell walls (Parsons 1981; Engelking et al. 2007). Therefore, the synthesis rates of newly formed fungal ^{15}N-GluN and bacterial ^{15}N-Mur during a short incubation period (hours to days) has been used to indicate the NO_3^- immobilization activities of fungi and bacteria, respectively (Li et al. 2019, 2020). Li et al. (2021) further developed a mathematical framework approach, in which the experimentally measurable gross microbial NO_3^- immobilization rates and the synthesis rates of newly formed fungal ^{15}N-GluN and ^{15}N-Mur are combined, to quantify soil NO_3^- immobilization rates by fungi and bacteria.

The subtropical montane areas of Southwest China are intensively used for agriculture (Zhou et al. 2012; Wang et al. 2017) and are hot spots of NO_3^- leaching loss that accounts for over 20% of the N inputs (Zhou et al. 2012). It is noteworthy that, in this region, a large area of sloping croplands was converted to orchards and woodlands in the last decades (Wang et al. 2017; Zhou et al. 2019), leading to a typical subtropical montane agricultural landscape that consists of a mosaic of different land uses (e.g., cropland, afforested woodland and orchard) rather than the agricultural landscape with an uniform of croplands. Therefore, investigating soil microbial NO_3^- immobilization across different land use types and along the whole soil profiles are vital to obtain the overall soil microbial NO_3^- immobilization and thereby developing soil management practices for NO_3^- retention at the landscape scale, especially for the mosaic montane agricultural landscape of Southwest China.

Based on the ^{15}N tracing and amino sugars-SIP techniques and in combination with the mathematical framework (Li et al. 2021), we quantified soil gross microbial NO_3^-

immobilization rates and the relative contribution of fungi and bacteria throughout the whole soil profile (0-60 cm) across three land use types in a subtropical mosaic montane agricultural landscape. We hypothesized that: 1) soil gross microbial NO_3^- immobilization rate might decrease along with the increases of land use management intensity and soil depth; 2) fungi might contribute more in immobilizing NO_3^- than bacteria do across different land uses and soil depths.

Materials and Methods.

Site description and soil sampling

This study was conducted at the Yanting Agro-Ecological Experimental Station of Purple Soil of the Chinese Academy of Sciences, Sichuan Province, Southwest China (31°16′N, 105°28′E). The climate is classified as moderate subtropical monsoon climate with an annual mean temperature of 17.3℃ and a mean precipitation of 826 mm, with approximately 70% of the annual precipitation occurring from May to September (Zhou et al. 2014). The soil is classified as a Pup-Orthic Entisol (Chinese Soil Taxonomy), Eutric Regosol (FAO Soil Classification), or Calcaric Leptic Cambisols (WRB Classification) (Meng et al. 2023), and it is derived from purplish shale that displays a typical "binary structure of soil-bedrock" (Zhou et al. 2012) (Fig. 1). The soils there are neutral or alkaline and therefore characterized by high autotrophic nitrification, leading to the production of NO_3^- (Wang et al. 2015; Zhang et al. 2022). NO_3^- accumulated in dry seasons was predominantly lost via subsurface flow in rainy seasons (Wang et al. 2011). Due to the shallow soil layers (20-80 cm) and the extremely poor water conductivity of the underlying parent bedrock beneath the soil (Zhou et al.

2012), NO_3^- could move downwards along the slope.

In the present study, three typical land use types (woodland, orchard and cropland) with three spatial replicates in a subtropical mosaic montane agricultural landscape were selected. The woodland sites have been afforested from slope cropland with cypress (*Cupressus funebris* Endl.) as the main stand species approximately 40 years ago (Zhou et al. 2019). The orchard sites have been established with citrus (*Citrus maxima* (Burm) Merr.) on the former croplands approximately 15 years ago. The cropland sites have been continuously cultivated with winter wheat (*Triticum aestivum* L.) and summer maize (*Zea mays* L.) rotation for over 20 years.

In January 2021, soil samples were taken at 60 cm in three successive soil depths: 0-20, 20-40, and 40-60 cm using an auger with a diameter of 3.6 cm from each replicated plot for each land use type. Three grids (4m×4 m) were randomly selected for sampling, and in total 12 soil cores were sampled for each replicate plot. Stones and roots were removed from the soil, and fresh soil was subsequently passed through a 2 mm sieve. Soil samples were then split into three subsamples. One subsample was stored at 4 °C for incubation experiments that started within one week after sampling, one subsample was stored at -20 ℃ for microbial PLFA biomass analysis, and one subsample was air-dried for the analysis of soil properties. The soil physicochemical properties for each land use type are shown in Table 1.

Determination of soil gross microbial NO_3^- immobilization rates

The soil gross microbial NO_3^- immobilization rates were quantified for each land use soil. 20 g of each fresh soil sample (oven-dried basis) was placed in a 250 ml flask and in total 108 flasks (3 land uses × 3 soil layers × 3 replicates × 4 sampling points) were included. After the flasks were covered with perforated parafilm (Parafilm M®, Bemis Company, Inc.), the soils (with average gravimetric water content of 21.7%) were pre-incubated in the dark at 25℃ for 1 day (Cheng et al. 2015; Chen et al. 2020). After the pre-incubation, 2 ml ^{15}N-enriched $K^{15}NO_3$ solution (10.158% atom) (Shanghai Engineering Research Center of Stable Isotope, Shanghai, China) (equivalent to 100 mg NO_3^--N kg^{-1} soil dry weight) was added to each soil sample by pipetting the solution uniformly over the soil surface. Subsequently, the final soil moisture was adjusted to 60% of the water-holding capacity (WHC) by adding deionized water (Chen et al. 2020). The flasks were then covered again with parafilm (Parafilm M®, Bemis Company, Inc.) and incubated in the dark at 25℃ for 7 days. To maintain soil water content, deionized water equivalent to the evaporation loss was added into the flasks when needed. At 0.5, 24, 72, and 144 h after ^{15}N labeling, soils were extracted with 100 ml 2 M KCl solution for 1 h at 300 rpm at 25℃ on a mechanical shaker, and then the extracts were filtered through Whatman filter papers (Ashless, diameter 90mm, CAT No. 1441-090, Whatman™) to determine the concentration and isotopic composition of NO_3^-. After the KCl extraction, deionized water was used to wash the residual soils until the NO_3^- contents in the water extracts below the detect limit, then the soils were oven-dried at 60℃ to a constant weight and ground to pass through a 0.15 mm sieve for the ^{15}N analysis of insoluble organic N (Wang et al. 2019; Chen et al. 2020).

The soil gross microbial NO_3^- immobilization rate (I_{NO3}) was calculated by the organic ^{15}N recovery method (Romero et al. 2015; Cheng et al. 2017; Wang et al. 2019; Chen et al. 2020). It is expressed as the differences in ^{15}N recovered in the KCl-extracted residue soil between 0.5 h and 144 h after ^{15}N addition divided by the total amount of labeled $^{15}NO_3^-$-N added:

$$\text{Org}\ ^{15}N_i = \text{Org}\ N_i \times Ae_{OrgaNi}, \quad (1)$$

$$I_{NO3} = \frac{1}{d}\sum_{i=1}^{n} \frac{Org^{15}N_{i+1} - Org^{15}N_i}{\frac{Ae_{i+1}+Ae_i}{2}} \quad (2)$$

where Org $^{15}N_i$ is the amount of ^{15}N in the KCl-extracted residue soil, d is the number of days of incubation, Org N_i is the measured amount of N in the washed soil residue, Ae_{OrgaNi} is the ^{15}N atom% excess in the washed soil residue, and Ae_i is the ^{15}N atom% excess of NO_3^-.

Determination of soil NO_3^- immobilization of fungi and bacteria

The synthesis rates of fungal-derived ^{15}N-GluN and ^{15}N-MurN in soils were determined for each land use. 10 g dry weight of each fresh soil sample was placed in a 60 ml flask. 27 flasks (3 land uses × 3 soil layers × 3 replicates) were included. The flasks were covered with perforated parafilm (Parafilm M®, Bemis Company, Inc.) and then soil samples (with average gravimetric water content of 21.7%) were pre-incubated in the dark at 25℃ for 1 day. After 1 day, 2 ml ^{15}N-enriched $K^{15}NO_3$ solution (99% atom) was added uniformly to each flask at a rate of 100 mg N kg^{-1} soil dry weight. The final soil moisture content was adjusted to 60% WHC. Subsequently, the soils were incubated for 7 days at 25 ℃. To maintain the soil moisture, deionized water was supplied daily to compensate for evaporative water loss. At the end of the incubation, soils were freeze-dried and ground to pass through a 0.25 mm sieve for the determination of amino sugar concentrations and ^{15}N isotope incorporation into amino sugars. The original soil samples were used as controls to obtain background values of the soil N isotopic signatures (Li et al. 2019, 2020). When $^{15}N\text{-}NO_3^-$ was assimilated into fungi and bacteria, the newly synthesized amino sugars (GluN and MurN) contained the heavy isotope (^{15}N) and thus could be differentiated from the old amino sugars. The proportion of ^{15}N-labeled GluN and MurN over the total amount of amino sugars was calculated as atom percentage excess (APE):

$$APE = (Re-Rc)/[1+(Re-Rc)]\times100 \qquad (3)$$

where Re is the isotope ratio of the incubated samples, Re = [A(F+1)/A(F)] (A is the area of the selected ion, F is the characteristic N-containing fragment, and F+1 indicate that only 1 N atom is included in an amino sugar molecule), and Rc is the corresponding ratio obtained from the original soil analyzed in the same GC/MS assay (He et al. 2006; Li et al. 2019, 2020).

The content of ^{15}N-labeled GluN and MurN was then calculated considering their respective concentration and APE (He et al. 2006, 2011):

$$CL = CT\times APE/100 \qquad (4)$$

where CL is the content of the ^{15}N-labeled portion of GluN and MurN, and CT is the concentration of each amino sugar measured by GC.

Theoretically, the molar ratio of GluN to MurN is 1:1 in bacterial peptidoglycan (Amelung 2001). However, because MurN breaks down faster than GluN and GluN occurs in bacterial products other than peptidoglycan (Amelung 2001; Joergensen and Wichern 2018), routinely a molar ratio of 2:1 (GluN: MurN) is used to calculate the bacterial-derived ^{15}N-GluN (B-^{15}N-GluN) (Engelking et al. 2007; Li et al. 2019, 2020). Fungal-derived ^{15}N-GluN (F-^{15}N-GluN) was calculated by subtracting B-^{15}N-GluN from the total ^{15}N-GluN. The synthesis rates of F-^{15}N-GluN and ^{15}N-MurN were applied to indicate fungal and bacterial NO_3^- immobilization activities in the studied soils, respectively.

Calculation of fungal and bacterial immobilization rates

The mathematical framework approach was employed to quantify the soil fungal and bacterial NO_3^- immobilization rates with the assumption that fungi and bacteria are the dominant participants in immobilizing NO_3^- in soils (Li et al. 2021). In brief, the soil gross NO_3^- immobilization rate obtained using the ^{15}N tracing method and synthesis rates of F-^{15}N-GluN and ^{15}N-MurN measured by the ^{15}N-amino sugar-SIP approach were utilized by the mathematical framework to estimate the conversion coefficients between the NO_3^- immobilization rates of fungi and bacteria and their respective cumulative rates of amino sugar-N. Thus, the respective soil fungal and bacterial NO_3^- immobilization rates were calculated according to the following equations:

$$F_{NO3} = K_F \times F \qquad (5)$$

and

$$B_{NO3} = K_B \times B \qquad (6)$$

where F_{NO3} and B_{NO3} is the respective fungal and bacterial NO_3^- immobilization rate; F and B is the synthesis rate of fungal-derived ^{15}N-GluN and bacterial-derived ^{15}N-MurN, respectively; K_F and K_B is the respective conversion coefficient from the fungal-derived ^{15}N-GluN synthesis rate to the fungal NO_3^- immobilization rate and the bacterial-derived ^{15}N-MurN synthesis rate to the bacterial NO_3^- immobilization rate.

According to the least-squares estimation, the conversion coefficients K_F and K_B were calculated using equation (7):

$$\widehat{K} = (X^T X)^{-1} X^T G \tag{7}$$

where $K = \begin{bmatrix} K_F \\ K_B \end{bmatrix}$, $X = \begin{bmatrix} F_1 & B_1 \\ F_2 & B_2 \\ F_3 & B_3 \end{bmatrix}$, $G = \begin{bmatrix} G_1 \\ G_2 \\ G_3 \end{bmatrix} = I_{NO3}$. The detailed calculation is in Appendix and more details can be found in Li et al. (2021).

The analysis of soil properties

SOC was determined by wet digestion with H_2SO_4-$K_2Cr_2O_7$ (Yeomans and Bremner 1988). Soil TN was determined by an elemental analyzer (vario MACRO cube, Elementar Analysensysteme GmbH, Langenselbold, Germany). Soil DOC was determined in an aqueous extract (4:1 water-to-soil ratio, v/w) using a continuous-flow auto analyzer (AA3, Bran Luebbe, Norderstedt, Germany). Soil ammonium (NH_4^+-N) and nitrate (NO_3^--N) were extracted using 2M KCl (soil: solution ratio = 1:5 w/v), and their concentrations in the extracts were determined spectrophotometrically (Dorich and Nelson 1983; Causse et al. 2017). Available P (AP) was extracted using 0.0125 M H_2SO_4 in 0.05 M HCl and quantified using the molybdenum blue method (Hylander et al. 1996). Soil MBC and MBN were analyzed using the chloroform fumigation-extraction method (Brookes et al. 1985). Soil cation exchange capacity (CEC) was determined using the hexamine cobalt trichloride solution spectrophotometric method (Nel et al. 2023). Soil pH was measured at a 1:2.5 (w: v) soil: water ratio with an mV/pH electrode (DMP-2, Quark Ltd, Nanjing, China).

Statistical analysis

Two-way analysis of variance (ANOVA) was used to determine the effects of land use type and soil depth on soil properties and soil gross microbial NO_3^- immobilization rates. One-way ANOVA was used to assess the differences soil fungal and bacterial NO_3^- immobilization rates among the different land use types. Duncan's multiple range test was applied to compare the means for the different treatments and rank them in descending order. The differences were considered statistically significant when $p < 0.05$. The matrix correlation was used to reveal the relationships between microbial NO_3^- immobilization rates and edaphic factors. Ridge regression analyses were employed to determine the most important environmental factors influencing microbial NO_3^- immobilization rates. Linear regression analyses were used to determine the relationships between soil fungal and NO_3^- immobilization rates and their respective PLFA biomass. Spearman correlation analyses were applied to determine the correlations between microbial PLFA biomass and environmental factors detected by the Mantel test in R. All statistical analyses were performed in R (R Core Development Team, R Foundation for Statistical Computing, Vienna, Austria).

Results

Soil physical-chemical and microbial properties

Soil properties of different land use types in soil profile were shown in Table 1. . The results of two-way ANOVA test (Table 1) showed that the soil properties differed among different land use types, which varied with soil depths. Overall, the SOC (4.71 - 30.59 g kg^{-1}), TN (0.37 - 1.96 g kg^{-1}), DOC (10.12 - 53.10 mg kg^{-1}), MBC (43.46 - 826.28 mg C kg^{-1}) and MBN (11.43 - 164.84 mg N kg^{-1}) concentrations as well as fungal PLFA biomass (1.26 - 10.75 n mol g^{-1}) and bacterial PLFA biomass (3.03 - 22.71 n mol g^{-1}) were significantly higher in woodland soils than those in orchard and cropland soils ($p < 0.05$). Besides, SOC, TN, DOC, NO_3^--N and AP, MBC, MBN, fungal and bacterial PLFA biomass gradually decreased with increasing soil depth for all land use types (Table 1; $p < 0.05$).

Soil gross microbial NO_3^- immobilization rates

Soil gross microbial NO_3^- immobilization rates varied across different land use types and soil layers (Fig. 2). For all land use types, soil gross microbial NO_3 immobilization rates for top soils (0-20 cm) were significantly higher than for subsoils (i.e., 20-40 cm, $p < 0.05$; Fig. 2). Notably, ^{15}N recoveries in 40-60 cm did not change significantly in all land use types (Fig. S1), and thus we failed to compute soil gross NO_3^- immobilization rates in 40-60 cm. The results of two-way ANOVA test showed that soil gross NO_3^- immobilization rates differed among different land use types ($p < 0.01$), which varied with soil depth. On average, soil gross microbial NO_3^- immobilization rates in woodland soils (145.69 μg N kg^{-1} soil d^{-1} for 0-20 cm and 44.06 μg N kg^{-1} soil d^{-1} for 20-40 cm) were significantly higher than those in orchard and cropland soils (Fig. 2). There were no significant differences in soil gross microbial NO_3^- immobilization rates for top soils between orchard soil (34.10 μg N kg^{-1} soil d^{-1}) and cropland soil (33.10 μg N kg^{-1} soil d^{-1}), while in 20-40cm, the soil gross microbial NO_3^--N immobilization rate in cropland soil (26.03 μg N kg^{-1} soil d^{-1}) was significantly higher than that in the orchard soil (15.75 μg N kg^{-1} soil d^{-1}) ($p < 0.05$, Fig. 2).

Soil fungal and bacterial NO_3^- immobilization

Soil fungal and bacterial NO_3^- immobilizations in subsoils were below the detection limit. In 0-20cm, the variations of fungal and bacterial NO_3^- immobilization rates across different land use soils were generally in consistent with their respective synthesis rate of F-^{15}N-GluN and ^{15}N-Mur (Fig. 3 and Fig. S2). Both soil fungal and bacterial NO_3^- immobilization rates in woodland soil were significantly higher than those in orchard and cropland soils ($p < 0.05$; Fig. 3). Soil fungal NO_3^- immobilization rate in orchard soil was significantly higher than that in cropland soil ($p < 0.05$), while no significant difference in soil bacterial NO_3^- immobilization rates between orchard and cropland soils was observed. Soil fungi played a greater role in assimilating soil NO_3^- in woodland and orchard soils ($p < 0.05$; Fig. 3), especially in woodland soil, where fungal NO_3^- immobilization rate was approximately twice as high as bacterial NO_3^- immobilization rate. In contrast, greater bacterial NO_3^- immobilization rate (18.53 μg N kg^{-1} soil d^{-1}) than fungal NO_3^- immobilization rate (12.25 μg N kg^{-1} soil d^{-1}) occurred in cropland soil.

Relationships between microbial NO_3^- immobilization rates and soil properties

Soil gross microbial NO_3 immobilization rates were significantly correlated with soil properties (Fig. 4a). Soil SOC, DOC, TN, C/N, MBC, and MBN together could explain over 90% of the variations in soil microbial NO_3^- immobilization rates across different land uses and soil layers ($p < 0.001$, Table 4). The ridge regression analysis suggested that over 84% of the variations in microbial NO_3^- immobilization rates in top soils (0-20 cm) could be explained by SOC, DOC, DOC/IN, and DOC/AP ($p = 0.018$, Table 2). Soil DOC, MBC, and CEC together could explain 85% of the variations in microbial

NO_3^- immobilization rates in subsoils (20-40 cm) (p = 0.005, Table 3). Moreover, over 85% of the variations in soil fungal and bacterial NO_3^- immobilization rates were explained by their respective PLFA biomass (p < 0.001, Fig. 7), which were significantly correlated with soil available P (AP) as well as the MBC/MBN, DOC/IN, and DOC/AP ratios (p < 0.05, Fig. 8).

Discussion

Comparisons of soil gross microbial NO_3^- immobilization rates with previous studies

SOC is one of the most important factors controlling the rates of soil microbial NO_3^- immobilization (Recous et al. 1990) and therefore, considering the relatively low SOC contents in the study region, we expected low gross microbial NO_3^- immobilization rates (15.8 - 145.7 μg N kg^{-1} soil d^{-1}), which was comparable with previous observations there in the same study area (Zhang et al. 2022) but lower than most of the available observations (3.80 to 6360.0 μg N kg^{-1} soil d^{-1}) (Table S1). The significantly positive correlation between soil gross microbial NO_3^- immobilization rates with SOC contents (Fig. 5) suggested that the high SOC content could provide enough organic C to satisfy the requirements of microbes to immobilize NO_3^- in soils (Schimel and Bennett 2004; Booth et al. 2005).

The SOC content was not the only soil property affecting soil microbial NO_3^- immobilization (Zhang et al. 2013a, b; Wang et al. 2015), because a significantly negative correlation between soil microbial NO_3^- immobilization rates and soil pH was found (Fig. 5g), and this explained the relatively low soil microbial NO_3^-

immobilization rates in our study as compared with those reported for acidic soils (Zhang et al. 2013b; Li et al. 2019) (Table S1). This is likely because the activities of fungi and soil enzymes (e.g., β-*N*-acetylglucosaminidase) decrease with the increase in soil pH (Sinsabaugh et al. 2008; Li et al. 2019). Moreover, the contents of soil DOC, MBC, and MBN as well as the C/N ratio were also controlling factors of soil microbial NO_3^- immobilization rates in the study (Table 4) as well as other different studies across the world (Fig. 5). The global meta-analysis also showed that high soil C and N availability and microbial activity increase soil microbial NO_3^- immobilization (Elrys et al. 2022). Therefore, managing soils in a way that supports C and N availability is crucial for the conversion of NO_3^- especially in calcareous subtropical montane soils (Hou et al. 2020).

Effects of land use on soil gross microbial NO_3^- immobilization rates

In the present study, soil microbial NO_3^- immobilization rates in woodland soils were significantly higher than those in orchard and cropland soils across different soil layers (Fig. 1). This is because both fungi and bacteria showed stronger immobilization of NO_3^- in woodland soils (Fig. 3; Fig. S2). The positive correlations between microbial PLFA biomass and soil C (e.g., SOC, DOC, MBC; Fig. 8) indicated that woodland soils favored more active fungal and bacterial biomass through higher C availability thus with greater N demand (Li et al. 2020). While in orchard and cropland soils, agricultural management practices are responsible for the decline of soil microbial NO_3^- immobilization (Frey et al. 1999; Six et al. 2006; Zhang, et al. 2013b; Xie et al. 2018; Li et al. 2019). For example, harvest-induced lower availability of bioavailable organic

C compounds (reflected e.g., in the DOC and MBC content; Table 1) in cropland and orchard soils could constrain the energy supply for microbial NO_3^- uptake, reduction, and assimilation processes (Wang et al. 2019). Our study demonstrated that agricultural practices decreased soil NO_3^- retention through reducing C substrates for microbes and inhibiting the function of fungi and bacteria.

Soil microbial NO_3^- immobilization rates for top soils (0-20 cm) were approximately 30-300% higher than those for subsoils (20-40 cm), while it could be ignored at the soil depth below 40 cm across different land use types (Fig. 2). The Mantel test indicated that the SOC, DOC, TN contents and MBC, MBN were the major regulators of soil microbial NO_3^- immobilization rates regardless of land use types (Fig. 4). As compared with deep soil layers, the top soils receive high inputs of organic C through plant litter and fine roots, which in turn provides enough bioavailable organic C substrates for stimulating soil microbial NO_3^- immobilization (Kummerow et al. 1982; da Silva Moco et al. 2009), and this explains the higher soil microbial NO_3^- immobilization rates in subsoils (20-40 cm) of woodland sites than those in top soils (0-20 cm) of both orchard and cropland sites (Fig. 2). These results indicated that subsoils cannot be ignored when assessing the overall microbial NO_3^- immobilization in particular for the areas with high C availability in the soil profile.

Contributions of fungi and bacteria in immobilizing soil NO_3^-

Fungi and bacteria contributed differently to NO_3^- immobilization across different land use types. In woodland soils, fungi dominated soil NO_3^- immobilization (approximately 2 times of bacterial NO_3^- immobilization) (Fig. 3), confirming what already reported in afforested woodland soils (e.g., Li et al. 2019). This may depend on: i) the lignocellulose-rich litter in woodland favors more of the development of fungal communities than bacterial communities (Deng et al. 2016; Gunina et al. 2017) due to the ability of fungi to degrade lignin (de Boer et al. 2005); ii) the C/N ratio of fungi is averagely higher than that of bacteria, and thus fungi preferentially decompose soil organic compounds of high C/N ratio to maintain their stoichiometric balance (Rousk and Bååth 2007; Yannikos et al. 2014), thereby leading to a greater utilization amount of soil NO_3^- by fungi than by bacteria. This interpretation is further supported by the significant positive relationship between the C/N ratio and fungal PLFA biomass in this study (Fig. 8). Overall, our results suggest that the ability of fungi to transform N-containing compounds may be a crucial driver of soil N cycling in woodland soils. Compared with woodland soils, the relative contribution of fungi to NO_3^- immobilization decreased more dramatically than that of bacteria in orchard and cropland soils (Fig. 3), indicating that fungal NO_3^- immobilization is more sensitive than bacterial NO_3^- utilization to agricultural practices, which is in line with Li et al. (2019), who found the decreased level of soil NO_3^- immobilization by fungi was 20% higher than that by bacteria following the conversion of woodland to agricultural soils. This phenomenon may depend on: i) bacteria may cope better with the declining availability of C resources in agricultural soils than fungi do, as demonstrated by the significant positive correlations between soil SOC and DOC contents with fungal biomass but not with bacterial biomass (Fig. 8); ii) fungal NO_3^- immobilization is not favorable in soils with high P availability (Giltrap and Lewis 1981; Nilsson and

Wallander 2003; Treseder 2004; Leff et al. 2015), while agricultural soils receive a large amount of P fertilizers to achieve high productivity and the high levels of soil P availability might have more constraining effects on the growth of fungi than that of bacteria, as indicated by the stronger negative relationships between AP with fungal biomass than with bacterial biomass (Fig. 8).

It is noteworthy that bacteria even played a greater role than fungi in immobilizing NO_3^- in cropland soils in the present study (Fig 3), which is inconsistent with our hypotheses and is contrary to Li et al. (2019). This difference might be explained by the variation of soil pH between our study (pH = 8.15) and theirs (pH = 4.97) because fungi are more favored in acidic soils (Blagodatskaya and Anderson 1998; Högber et al. 2007). Nevertheless, there were also investigations reporting that bacteria is more important than fungi in immobilizing soil NO_3^- (Myrold and Posavatz 2007; Boyle et al. 2008). Fungi prefer living in physically undisturbed soils because of their hyphal networks (Blagodatskaya and Anderson 1998; Högberg et al. 2007). Thus, tillage at the cropland sites might have destroyed the hyphal networks (Helgason et al. 1998; Högberg et al. 2003; de Vries et al. 2007; Roger-Estrade et al. 2010) and thereby decreasing fungal NO_3^- immobilization. In addition, Strickland and Rousk (2010) have demonstrated that, as compared with fungi, bacteria may exhibit stronger assimilation of soil NO_3^- due to its higher biomass in soils. Thus the significantly higher ratios of bacterial PLFA biomass to fungal PLFA biomass in cropland soils (3.0) than woodland (2.1) and orchard (2.4) soils may explain the more important roles of bacteria than fungi in soil microbial NO_3^- immobilization in the present study. This interpretation could be further proved by the fact that bacterial NO_3^- immobilization rate (2.94 g N mol^{-1} d^{-1}) was significantly lower than fungal NO_3^- immobilization rate (5.85 g N mol^{-1} d^{-1}) in cropland soils (Fig S3; $p < 0.05$), which indicated that the higher bacterial NO_3^- immobilization rate was probably the results of higher bacterial biomass. Simultaneously, the inconsistency between microbial NO_3^- immobilization rates and intensities indicated that the variations of fungal and bacterial NO_3^- immobilization between different land uses were not only caused by differences in PLFA-derived biomass, but also by different fungal and bacterial species (Carey 2016; Fierer 2017). Thus, future studies on soil microbial NO_3^- immobilization should consider the composition of fungal and bacterial communities (Lauber et al. 2008; Li et al. 2020).

Conclusion

The soil gross microbial NO_3^- immobilization rates were significantly higher than in orchard and cropland soils across different soil layers, and the topsoil (0-20 cm) was the dominant layer for soil microbial NO_3^- immobilization across different land use types but the roles of subsoils (e.g., 20-40 cm) cannot be ignored especially for subsoils with high bioavailable organic compounds. Soil fungi was more important than bacteria in immobilizing NO_3^- in woodland and orchard soils while the opposite occurred in cropland soil, likely due to the relative contribution of fungal and bacterial biomass across different land use types. Our observations provide a mechanistic understanding of how and why soil microbial NO_3^- immobilization varies across different land use types in a subtropical mosaic montane agricultural landscape characterized by alkaline soils. Nevertheless, some limitations exist in our study. First, we failed to quantify fungal and bacterial NO_3^- immobilization rates in subsoils (e.g., 20-40cm) due to the weak NO_3^- immobilization by microbes and methodological limitation. Second, the absence of plants in our incubation experiments may limit our understandings of the underlying mechanisms of the interactions between plant and microorganisms and avoid to generalize these results. Future studies to mimic in situ conditions (e.g., undisturbed intact soils and plant growth) are needed to further improve the understanding of the underlying mechanisms of microbial NO_3^- immobilization in various ecosystems.

Acknowledgement

This study was supported by the National Natural Science Foundation of China (Grant No. U20A20107; U22A20562).

Declarations

Conflict of interest: The authors declare no competing interests.

References

Allen K, Corre MD, Tjoa A, Veldkamp E (2015) Soil nitrogen-cycling responses to conversion of lowland forests to oil palm and rubber plantations in sumatra, indonesia. PLoS One 10: e0133325

Amelung W (2001) Methods using amino sugars as markers for microbial residues in soil. In: Lal R, Kimble JM, Follett RF, Stewart BA (eds) Assessment methods for soil carbon. Lewis Publishers, Boca Raton, pp 233–272

Banning NC, Grant CD, Jones DL, Murphy DV (2008) Recovery of soil organic matter, organic matter turnover and nitrogen cycling in a post-mining forest rehabilitation chronosequence. Soil Biol Biochem 40:2021-2031

Bijay-Singh, Craswell E (2021) Fertilizers and nitrate pollution of surface and ground water: an increasingly pervasive global problem. SN Applied Sciences 3:1-24

Blagodatskaya EV, Anderson TH (1998) Interactive effects of pH and substrate quality on the fungal-to-bacterial ratio and qCO_2 of microbial communities in forest soils. Soil Biol Biochem 30:1269-1274

Booth MS, Stark JM, Rastetter E (2005) Controls on nitrogen cycling in terrestrial ecosystems: a synthetic analysis of literature data. Ecol Monogr 75:139-157

Bottomley PJ, Taylor AE, Myrold DD (2012) A consideration of the relative contributions of different microbial subpopulations to the soil N cycle. Front Microbiol 3:373

Boyle SA, Yarwood RR, Bottomley PJ, Myrold DD (2008) Bacterial and fungal contributions to soil nitrogen cycling under Douglas fir and red alder at two sites in Oregon. Soil Biol Biochem 40:443-451

Brookes PC, Landman A, Pruden G, Jenkinson DS (1985) Chloroform fumigation and the release of soil nitrogen - a rapid direct extraction method to measure microbial biomass nitrogen in soil. Soil Biol Biochem 17:837-842

Carey J (2016) News feature: crucial role of belowground biodiversity. PNAS 113:7682-7685

Causse J, Thomas O, Jung AV, Thomas MF (2017) Direct DOC and nitrate determination in water using dual pathlength and second derivative UV spectrophotometry. Water Res 108: 312-319

Chang RY, Fu BJ, Liu GH, Wang S, Yao XL (2012) The effects of afforestation on soil organic and inorganic carbon: A case study of the Loess Plateau of China. Catena 95:145-152

Chen ZX, Zhang HM, Tu XS, Sun X, Wang J, Cheng Y, Zhang JB, Cai ZC, Chang SX (2020) Characteristics of organic material inputs affect soil microbial NO_3^- immobilization rates calculated using different methods. Eur J Soil Sci 72:480-486

Cheng Y, Zhang JB, Müller C, Wang SQ (2015) ^{15}N tracing study to understand the N supply associated with organic amendments in a vineyard soil. Biol Fertil Soils 51:983-993

Cheng Y, Wang J, Wan JY, Chang SX, Wang SQ (2017) The quality and quantity of exogenous organic carbon input control microbial NO_3^- immobilization: A meta-analysis. Soil Biol Biochem 115:357-363

Cheshire MV, Bedrock CN, Williams BL, Chapman SJ, Solntseva I, Thomsen I (1999) The immobilization of nitrogen by straw decomposing in soil. Eur J Soil Sci 50:329-341

Cui SH, Shi YL, Groffman PM, Schlesinger H, Zhu YG (2013) Centennial-scale analysis of the creation and fate of reactive nitrogen in China (1910-2010). PNAS 110:2052-2057

da Silva Moco MK, da Gama-Rodrigues EF, da Gama-Rodrigues AC, Machado RCR, Baligar VC (2009) Soil and litter fauna of cacao agroforestry systems in Bahia, Brazil. Agroforest Syst 76:127-138

de Boer W, Folman LB, Summerbell RC, Boddy L (2005) Living in a fungal world: impact of fungi on soil bacterial niche development. FEMS Microbiol Rev 29:795-811

de Vries FT, Bloem J, van Eekeren N, Brusaard L, Hoffland E (2007) Fungal biomass in pastures increases with age and reduced N input. Soil Biol Biochem 39:1620-1630

de Vries FT, van Groenigen JW, Hoffland E, Bloem J (2011) Nitrogen losses from two grassland soils with different fungal biomass. Soil Biol Biochem 43:997-1005

de Vries FT, Bardgett RD (2012) Plant-microbial linkages and ecosystem nitrogen retention: lessons for sustainable agriculture. Front Ecol Environ 10:425-432

Deng Q, Cheng XL, Hui DF, Zhang QA, Li M, Zhang QF (2016) Soil microbial community and its interaction with soil carbon and nitrogen dynamics following afforestation in central China. Sci Total Environ 541:230-237

Derrien D, Amelung W (2011) Computing the mean residence time of soil carbon fractions using stable isotopes: impacts of the model framework. Eur J Soil Sci 62:237-252

Dorich RA, Nelson DW (1983) Direct colorimetic measurement of ammonium in KCl extrcts of soils. Soil Sci Soc Am J 47:833-836

Elrys AS, Chen ZX, Wang J, Uwiragiye Y, Helmy AM, Desoky EM, Cheng Y, Zhang JB, Cai ZC, Müller C (2022) Global patterns of soil gross immobilization of ammonium and nitrate in terrestrial ecosystems. Global Change Biol 28:4472-4478

Engelking B, Flessa H, Joergensen RG (2007) Shifts in amino sugar and ergosterol contents after addition of sucrose and cellulose to soil. Soil Biol Biochem 39:2111-2118

Fierer N (2017) Embracing the unknown: disentangling the complexities of the soil microbiome. Nat Rev Microbiol. 15:579-590

Frey SD, Elliott ET, Paustian K (1999) Bacterial and fungal abundance and biomass in conventional and no-tillage agroecosystems along two climatic gradients. Soil Biol Biochem 31:573-585

Giltrap NJ, Lewis DH (1981) Inhibition of growth of ectomycorrhizal fungi culture by phosphate. New Phytol 87:669-675

Glaser B, Millar N, Blum H (2006) Sequestration and turnover of bacterial- and fungal-derived carbon in a temperate grassland soil under long-term elevated atmospheric pCO_2. Global Change Biol 12:1521-1531

Gunina A, Dippold M, Glaser B, Kuzyakov Y (2017) Turnover of microbial groups and cell components in soil: ^{13}C analysis of cellular biomarkers. Biogeosciences 14:271-283

He HB, Xie HT, Zhang XD (2006) A novel GC/MS technique to assess ^{15}N and ^{13}C incorporation into soil amino sugars. Soil Biol Biochem 38:1083-1091

He HB, Zhang W, Zhang XD, Xie HT, Zhuang J (2011) Temporal responses of soil microorganisms to substrate addition as indicated by amino sugar differentiation. Soil Biol Biochem 43:1155-1161

Helgason T, Daniell TJ, Husband R, Fitter AH, Young JPW (1998) Ploughing up the wood-wide web? Nature 394:431-431

Högberg MN, Bååth E, Nordgren A, Arnebrant K, Högberg P (2003) Contrasting effects of nitrogen availability on plant carbon supply to mycorrhizal fungi and saprotrophs – a hypothesis based on field observations in boreal forest. New Phytol 160:225-238

Högberg MN, Högberg P, Myrold DD (2007) Is microbial community composition in boreal forest soils determined by pH, C-to-N ratio, the trees, or all three? Oecologia 150:590-601

Hou D, Bolan NS, Tsang D, Kirkham MB, O'Connor D (2020) Sustainable soil use and management: An interdisciplinary and systematic approach. Sci Total Environ 729,138961

Huygens D, Boeckx P, Templer PH, Paulino L, Van Cleemput O, Oyarzún C, Müller C, Godoy R (2008) Mechanisms for retention of bioavailable nitrogen in volcanic rainforest soils. Nat Geosci 1:543-548

Hylander LD, Svensson HI, Siman G (1996) Different methods for determination of plant available soil phosphorus. Commun Soil Sci Plan 27:1501-12

Joergensen RG, Wichern F (2018) Alive and kicking: why dormant soil microorganisms matter. Soil Biol Biochem 116:419-430

Jones DL, Cooledge EC, Hoyle FC, Griffiths RI, Murphy DV (2019) pH and exchangeable aluminum are major regulators of microbial energy flow and carbon use efficiency in soil microbial communities. Soil Biol Biochem 138:107584

Kummerow J, Kummerow M, Dasilva WS (1982) Fine-root growth dynamics in cacao (*Theobroma cacao*). Plant Soil 65:193-201

Lauber CL, Strickland MS, Bradford MA, Fierer N (2008) The influence of soil properties on the structure of bacterial and fungal communities across land-use types. Soil Biol Biochem 40:2407-2415

Leff JW, Jone SE, Prober, SM, Barberán A, Borer ET, Firn JL, Harpole WS, Hobbie SE, Hofmockel KS, Knops JMH, McCulley RL, La Pierre K, Risch AC, Seabloom EW, Schütz M, Steenbock C, Stevens CJ, Fierer N (2015) Consistent responses of soil microbial communities to elevated nutrient inputs in grasslands across the globe. PNAS 112:10967-10972

Li XB, He HB, Zhang XD, Yan XY, Six J, Cai ZC, Barthel M, Zhang JB, Necpalova M, Ma QQ, Li ZA (2019) Distinct responses of soil fungal and bacterial nitrate immobilization to land conversion from forest to agriculture. Soil Biol Biochem

134:81-89

Li XB, Li ZA, Zhang XD, Xia LL, Zhang WX, Ma QQ, He HB (2020) Disentangling immobilization of nitrate by fungi and bacteria in soil to plant residue amendment. Geoderma 374:114450

Li XB, He HB, Zhang XD, Kazanci C, Li ZA, Necpalova M, Ma QQ (2021) Calculation of fungal and bacterial inorganic nitrogen immobilization rates in soil. Soil Biol Biochem 153: 108114

Manoharan L, Kushwaha SK, Ahren D, Hedlund K (2017) Agricultural land use determines functional genetic diversity of soil microbial communities. Soil Biol Biochem 115:423-432

Marzluf GA (1997) Genetic regulation of nitrogen metabolism in the fungi. Microbiol Mol Biol R 61:17-32

Meng Q, Li S, Liu B, Hu J, Liu JY, Chen YY, Ci E (2023) Appraisal of soil taxonomy and the world reference base for soil resourcesapplied to classify purple soils from the eastern Sichuan Basin, China. Agronomy-Basel 13:1837

Myrold DD, Posavatz NR (2007) Potential importance of bacteria and fungi in nitrate assimilation in soil. Soil Biol Biochem 39:1737-1743

Nel T, Bruneel Y, Smolders E (2023) Comparisons of five methods to determine the cation exchange capacity of soil. J. Plant. Nutr. Soil Sci. 186:311-320

Nelson MB, Martiny AC, Martiny JBH (2016) Global biogeography of microbial nitrogen-cycling traits in soil. PNAS 113:8033-8040

Nilsson LO, Wallander H (2003) Production of external mycelium by ectomycorrhizal fungi in a Norway spruce forest was reduced in response to nitrogen fertilization. New Phytol 158:409-416

Parsons JW (1981) Chemistry and distribution of amino sugars in soils and soil organisms In: Paul, EA, JNL (Eds), Soil Biochemistry Marcel Dekker, New York, 197-227

Recous S, Mary B, Faurie G (1990) Microbial immobilization of ammonium and nitrate in cultivated soils. Soil Biol Biochem 22:913-922

Rice CW, Tiedje JM (1989) Regulation of nitrate assimilation by ammonium in soils and in isolated soil microorganisms. Soil Biol Biochem 21:597-602

Roger-Estrade J, Anger C, Bertrand M, Richard G (2010) Tillage and soil ecology: partners for sustainable agriculture. Soil Till Res 111:33-40

Romero CM, Engel R, Chen C, Wallander R (2015) Microbial immobilization of nitrogen-15 labelled ammonium and nitrate in an agricultural Soil. SSSAJ 79:595-602

Rousk J, Bååth E (2007) Fungal and bacterial growth in soil with plant materials of different C/N ratios. FEMS Microbiol Ecol 62:258-267

Rousk J, Bååth E, Brookes PC, Lauber CL, Lozupone C, Gregory Caporaso J, Knight R, Fierer N (2010) Soil bacterial and fungal communities across a pH gradient in an arable soil. ISME J 4 :1340-1351

Schimel JP, Bennett J (2004) Nitrogen mineralization: challenges of a changing paradigm. Ecology 85:591-602

Sebilo M, Mayer B, Nicolardot B, Pinay G, Mariotti A (2013) Long-term fate of nitrate fertilizer in agricultural soils. PNAS 110:18185-18189

Shi W, Norton JM (2000) Microbial control of nitrate concentrations in an agricultural soil treated with dairy waste compost or ammonium fertilizer. Soil Biol Biochem 32:1453-1457

Sinsabaugh RL, Lauber CL, Weintraub MN, Ahmed B, Allison SD, Crenshaw C, Contosta AR, Cusack D, Frey S, Gallo ME, Gartner TB, Hobbie SE, Holland K, Keeler BL, Powers JS, Stursova M, Takacs-Vesbach C, Waldrop MP, Wallenstein MD, Zak DR, Zeglin LH (2008). Stoichiometry of soil enzyme activity at global scale. Ecol Lett 11:1252-1264

Six J, Frey SD, Thiet RK, Batten KM (2006) Bacterial and fungal contributions to carbon sequestration in agroecosystems. SSSAJ 70:555-569

Stark JM, Hart SC (1997) High rates of nitrification and nitrate turnover in undisturbed coniferous forests. Nature 385:61-64

Strickland MS, Rousk J (2010) Considering fungal:bacterial dominance in soils - methods, controls, and ecosystem implications. Soil Biol Biochem 42:1385-1395

Tahovská K, Kaňa J, Bárta J, Oulehle F, Richter A, Šantrůčková H (2013) Microbial N immobilization is of great importance in acidified mountain spruce forest soils. Soil Biol Biochem 59:58-71

Treseder KK (2004) A meta-analysis of mycorrhizal responses to nitrogen, phosphorus, and atmospheric CO_2 in field studies. New Phytol 164:347-355

Vázquez E, Benito M, Navas M, Espejo R, Díaz-Pinés E, Teutscherova N (2019) The interactive effect of no-tillage and liming on gross N transformation rates during the summer fallow in an acid Mediterranean soil. Soil Tillage Res 194:104297

Vitousek PM, Aber JD, Howarth RW, Likens GE, Matso PA, Schindler, DW, Schlesinger WH, Tilman D (1997) Human alteration of the global nitrogen cycle: sources and consequences. Ecol Appl 7:737-750

Wang J, Zhu B, Zhang JB, Müller C, Cai ZC (2015) Mechanisms of soil N dynamics following long-term application of organic fertilizers to subtropical rain-fed purple soil in China. Soil Biol Biochem 91:222-231

Wang J, Su N, Xu, MG, Wang SQ, Zhang JB, Cai ZC, Cheng Y (2019) The influence of long-term animal manure and crop residue application on abiotic and biotic N immobilization in an acidified agricultural soil. Geoderma 337:710-717

Wang T, Zhu B (2011) Nitrate loss via overland flow and interflow from a sloped farmland in the hilly area of purple soil, China. Nutr Cycl Agroecosys 90:309-319

Wang XG, Zhou MH, Li T, Ke Y, Zhu B (2017) Land use change effects on ecosystemcarbon budget in the Sichuan Basin of Southwest China: conversion of cropland to forest ecosystem. Sci Total Environ 609:556-562

Xie Y, Yang L, Zhu TB, Yang H, Zhang JB, Yang JL, Cao JH, Bai B, Jiang ZC, Liang YM, Lan FN, Meng L, Müller C (2018) Rapid recovery of nitrogen retention capacity in a subtropical acidic soil following afforestation. Soil Biol Biochem 120:171-180

Yannikos N, Leinweber P, Helgason BL, Baum C, Walley FL, Van Rees KCJ (2014)

Impact of Populus trees on the composition of organic matter and the soil microbial community in Orthic Gray Luvisols in Saskatchewan (Canada). Soil Biol Biochem 70:5-11

Yeomans JC, Bremner JM (1988) A rapid and precise method for routine determination of organic-carbon in soil. Commun Soil Sci Plan 19:1467-76

Yokobe T, Hyodo FJ, Tokuchi N (2020) Volcanic deposits affect soil nitrogen dynamics and fungal-bacterial dominance in temperate forests. Soil Biol Biochem 150: 108011

Zhang BW, Zhou MH, Zhu B, Xiao QY, Zheng XH, Zhang JB, Müller C, Butterbach-Bahl K (2022) Soil clay minerals: an overlooked mediator of gross N transformations in Regosolic soils of subtropical montane landscapes. Soil Biol Biochem 168:108612

Zhang JB, Cai ZC, Zhu TB, Yang WY, Müller C (2013a) Mechanisms for the retention of inorganic N in acidic forest soils of southern China. Sci Rep 3:2342

Zhang JB, Zhu TB, Meng TZ, Zhang YC, Yang JJ, Yang WY, Müller C, Cai ZC (2013b) Agricultural land use affects nitrate production and conservation in humid subtropical soils in China, Soil Biol Biochem 62:107-114

Zhang XD, Amelung W (1996) Gas chromatographic determination of muramic acid, glucosamine, mannosamine, and galactosamine in soils. Soil Biol Biochem 28:1201-1206

Zhou JY, Gu BJ, Schlesinger WH, Ju XT (2016) Significant accumulation of nitrate in Chinese semi-humid croplands. Sci Rep 6:25088

Zhou MH, Zhu B, Butterbach-Bahl K, Wang T, Bergmann J, Brüggemann N, Wang ZH, L TK, Kuang, FH (2012) Nitrate leaching, direct and indirect nitrous oxide fluxes from sloping cropland in the purple soil area, southwestern China. Environ Pollut 162:361-368

Zhou MH, Zhu B, Butterbach-Bahl K, Wang XG, Zheng XH (2014) Nitrous oxide emissions during the non-rice growing seasons of two subtropical rice-based rotation systems in southwest China. Plant Soil 383:401-414

Zhou MH, Wang XG, Ren X, Zhu B (2019) Afforestation and deforestation enhanced soil CH_4 uptake in a subtropical agricultural landscape: evidence from multi-year and multi-site field experiments. Sci Total Environ 662:313-23

Zogg GP, Zak DR, Pregitzer KS, Burton AJ (2000) Microbial immobilization and the retention of anthropogenic nitrate in a northern hardwood forest. Ecology 81:1858-1866

Table captions

Table 1. Soil physical, chemical and microbial properties under woodland, orchard and cropland soils in Yanting county of Sichuan province, China.

Table 2. Ridge regression analysis of soil properties to gross microbial NO_3^- immobilization rates in 0-20cm soil depth. Parameter Estimates (n = 9).

Table 3. Ridge regression analysis of soil properties to gross microbial NO_3^- immobilization rates in 20-40cm soil depth. Parameter Estimates (n = 9).

Table 4. Ridge regression analysis of soil properties to gross microbial NO_3^- immobilization rates in 0-20 and 20-40cm soil depth. Parameter Estimates (n = 18).

Table 1

Parameters		SOC (g kg^{-1})	TN (g N kg^{-1})	C/N ratio	DOC (mg kg^{-1})	NH_4^+ (mg N kg^{-1})	NO_3^- (mg N kg^{-1})	pH	CEC (c mol. kg^{-1})	TK (g kg^{-1})	TP (g kg^{-1})	AP (mg kg^{-1})	Clay (%)	MBC (mg C kg^{-1})	MBN (mg N kg^{-1})	Fungal PLFA biomass (n mol. g^{-1})	Bacterial PLFA biomass (n mol. g^{-1})	MBC/MBN	DOC/IN	DOC/AP
	0-20cm	30.59±3.34Aa	1.96±0.10Aa	15.14±2.11Aa	53.10±3.56Aa	2.73±0.66Aa	5.11±1.81Ba	8.02±0.41Bb	29.26±1.90Aa	29.99±6.60Aa	0.15±0.01Ba	2.65±0.44Ca	17.24±0.01Ab	826.28±56.00Aa	164.84±14.18Aa	10.75±1.68Aa	22.71±4.01Aa	5.02±0.07Aa	6.93±1.58Aa	20.24±1.99Aa
Woodland	20-40cm	5.41±0.43Ab	0.46±0.00Bb	11.77±0.95Aa	24.59±1.38Ab	1.97±0.50Aab	0.28±0.00Cb	8.36±0.06Aa	24.69±2.88Aa	32.26±9.01Aa	0.17±0.02Ba	1.06±0.35Bb	17.95±1.08Ab	147.16±34.42Ab	35.58±18.40Ab	1.26±0.46Ab	4.31±0.95Ab	4.52±1.20Aa	8.27±2.30Aa	18.81±1.25Aa
	40-60cm	4.71±1.48Ab	0.37±0.14Ab	14.12±6.22Aa	10.12±3.16Bc	1.48±0.33Ab	0.14±0.00Cb	8.37±0.02Aa	28.93±2.16Aa	36.75±0.90Aa	0.14±0.05Aa	0.96±0.10Bb	20.53±1.15Aa	43.46±5.48Ac	11.43±6.13ABb	1.26±0.42Ab	3.03±0.67Ab	2.59±0.47Ab	6.20±1.13Aa	10.88±4.71Ab
	0-20cm	7.62±0.68Ba	0.76±0.07Ba	10.08±0.17Ba	24.90±3.31Ba	0.57±0.20Bb	8.23±2.25Ba	8.16±0.06Ab	15.91±1.19Ca	31.26±6.82Aa	0.19±0.06Ba	14.05±1.70Ba	16.24±0.01Ba	115.78±22.86Ba	45.65±19.43Ba	3.59±0.42Ba	6.36±0.48Ba	2.85±1.13Ba	2.88±0.31Ba	1.78±0.23Bb
Orchard	20-40cm	5.41±2.60Aab	0.42±0.05Bb	9.68±0.58Ba	13.43±1.71Cb	1.40±0.48ABa	5.48±0.58Bb	8.22±0.07Bb	16.01±1.20Ba	24.63±6.04Aa	0.17±0.02Ba	2.00±0.10Bb	18.39±1.55Aa	54.75±4.06Bb	27.21±4.99Aab	1.18±0.49Ab	4.32±01.81Aa	2.04±0.24Ba	2.67±0.69Ba	6.75±1.14Ba
	40-60cm	3.62±0.91Ab	0.33±0.04Ab	10.77±1.67ABa	11.08±1.40ABb	1.08±0.13Aab	2.82±0.11Bb	8.37±0.05Aa	15.54±0.85Ca	25.50±2.26Ba	0.17±0.02Aa	1.36±0.10Ab	18.79±2.06Aa	52.14±6.19Ab	19.97±2.44Ab	0.33±0.24Bc	1.83±0.67Ab	2.62±0.38Aa	2.83±0.35Ba	8.16±21.33Aa
	0-20cm	5.10±0.51Ba	0.81±0.01Ba	6.30±0.63Ca	11.93±0.84Cc	3.05±0.35Aa	45.91±9.03Aa	7.91±0.04Cc	19.44±1.90Ba	35.06±5.34Aa	0.29±0.05Aa	21.52±3.34Aa	17.31±0.27Aa	173.16±16.36Ba	63.07±24.36Ba	2.13±0.31Ba	6.35±0.65Ba	3.04±1.23Ba	0.25±0.06Cc	0.59±0.14Bc
Cropland	20-40cm	3.64±0.36Ab	0.60±0.04Ab	6.11±0.88Ca	18.34±1.52Ba	0.63±0.08Bb	20.55±3.31Ab	8.20±0.04Bb	22.90±1.46Aa	38.20±4.15Aa	0.22±0.02Ab	8.92±1.66Ab	17.65±0.81Aa	68.82±9.34Bb	39.70±5.77Aab	0.71±0.44Ab	3.11±0.73Ab	1.57±0.19Ba	0.74±0.17Bb	2.11±0.44Cb
	40-60cm	2.54±0.85Ab	0.44±0.06Ac	5.64±1.09Ba	14.35±0.67Ab	0.61±0.05Bb	5.74±0.67Ac	8.38±0.04Aa	22.32±3.36Ba	24.57±3.79Bb	0.14±0.03Ac	1.41±0.17Ac	20.33±4.56Aa	11.96±6.14Bc	12.34±1.99Bb	0.43±0.21Bb	2.45±0.78Ab	0.97±0.26Bb	2.27±0.23Ba	10.28±0.94Aa
ANOVA (*p*-value)																				
land use type		0.000^{***}	0.000^{***}	0.000^{***}	0.000^{***}	0.000^{***}	0.000^{***}	0.001^{**}	0.000^{***}	0.067	0.003^{**}	0.000^{***}	0.65	0.000^{***}	0.000^{***}	0.000^{***}	0.000^{***}	0.000^{***}	0.000^{***}	0.000^{***}
soil depth		0.000^{***}	0.000^{***}	0.477	0.000^{***}	0.000^{***}	0.000^{***}	0.000^{***}	0.536	0.438	0.006^{**}	0.000^{***}	0.011^{*}	0.000^{***}	0.000^{***}	0.000^{***}	0.000^{***}	0.001^{**}	0.528	0.054
land use type × soil depth		0.000^{***}	0.000^{***}	0.706	0.000^{***}	0.000^{***}	0.000^{***}	0.000^{***}	0.034^{*}	0.033^{*}	0.021^{*}	0.000^{***}	0.806	0.000^{***}	0.000^{***}	0.000^{***}	0.000^{***}	0.046^{*}	0.061	0.000^{***}

Note: Different capital letters within the same column indicate significant differences between mean values among soils of different land uses for the same soil layer at $p < 0.05$. Different lowercase letters within the same column indicate significant differences in mean values among different soil layers under the same land use at $p < 0.05$. CEC, cation exchangeable capacity; AP, available P; MBC, microbial biomass C; MBN, microbial biomass N; MBC/MBN, ratio of microbial biomass C and N; DOC/IN, the ratio of dissolved organic C and sum of NH_4^+-N with NO_3^--N; DOC/AP, the ratio of dissolved organic C and available P. Data were presented as means of three replicates ± standard error; $^{*}p < 0.05$; $^{**}p < 0.01$; $^{***}p < 0.001$.

Table 2

	Unstandardized Coefficients		Standardized Coefficients	t	p	AdjR^2	F
	B	Std. Error	*Beta*				
Constant	19.032	10.754	-	1.770	0.151	0.841	P=0.018
SOC	0.581	0.092	0.217	6.291	0.003**		
DOC	0.568	0.104	0.185	5.484	0.005**		
DOC/IN	2.954	0.802	0.158	3.684	0.021*		
DOC/AP	1.369	0.251	0.233	5.445	0.006**		

Dependent variable: Gross microbial NO_3^- immobilization rates; *p<0.05 **p<0.01. SOC is soil organic C; DOC is dissolved organic C; DOC/IN is the ratio of dissolved organic C to inorganic N (NH_4^+-N plus NO_3^--N); DOC/AP is the ratio of dissolved organic C to available P.

Table 3

	Unstandardized Coefficients		Standardized Coefficients	t	p	AdjR^2	F
	B	Std. Error	*Beta*				
Constant	-6.848	5.678	-	-1.206	0.282	0.848	P=0.005
DOC	0.787	0.124	0.311	6.344	0.001**		
MBC	0.072	0.017	0.264	4.275	0.008**		
CEC	0.673	0.196	0.229	3.425	0.019*		

Dependent variable: Gross microbial NO_3^- immobilization rates; *p<0.05 **p<0.01. DOC is dissolved organic C; MBC is microbial biomass C; CEC is soil cation exchange capacity.

Table 4

	Unstandardized Coefficients		Standardized Coefficients	t	p	AdjR^2	F
	B	Std. Error	*Beta*				
Constant	-6.814	6.230	-	-1.094	0.297	0.905	P=0.000

SOC	0.421	0.040	0.159	10.474	0.000^{**}
TN	12.556	1.617	0.150	7.766	0.000^{**}
C/N	1.249	0.442	0.092	2.828	0.016^{*}
DOC	0.541	0.071	0.171	7.604	0.000^{**}
MBC	0.026	0.003	0.162	10.423	0.000^{**}
MBN	0.121	0.020	0.135	6.119	0.000^{**}

Dependent variable: Gross microbial NO_3^- immobilization rates; *p<0.05 **p<0.01. SOC is soil organic C; TN is total N; C/N is the ratio of C to N; DOC is dissolved organic C; MBC is microbial biomass C; MBN is the microbial biomass N.

Figure captions

Figure 1. The overhead view of the typical mosaic montane agricultural landscape (a), the soil profile – "binary structure of soil-bedrock" (b), and schematic illustration of the landscape profile in the study site (c).

Figure 2. Gross microbial NO_3^- immobilization rates in soils of different land uses. Different capital letters on the error bars denote significant differences in mean values of soils taken from different land uses in the same soil layer, while different lowercase letters denote significant differences in mean values between soil layers of the same land use ($p < 0.05$). Error bars are standard deviations of the mean (n = 3). The invisible error bars are smaller than the symbols.

Figure 3. fungal and bacterial immobilization rates of soil NO_3^- under different land use soils in the surface soil (0-20cm). Different letters denote significant differences in the average values among different land use soils at $p < 0.05$. Error bars are standard deviations of the mean (n=3). The invisible error bars are smaller than the symbols.

Figure 4. Relationships between gross microbial immobilization rates of soil NO_3^- and edaphic properties in the 0-20cm soil layer (a), 20-40cm soil layer (b), 0-20 and 20-40cm soil layers (c).

Figure 5. Relationships of gross microbial NO_3^- immobilization rates (I_{NO3}) with the contents of SOC, TN, DOC, MBC, MBN, the ratio of C/N and pH (N is the number of data pairs from Table S2)

Figure 6. Relationships between fungal and bacterial immobilization rates of soil NO_3^- and edaphic properties in the surface soil (0-20cm). F_{NO3} is fungal NO_3^- immobilization rate, B_{NO3} is bacterial NO_3^- immobilization rate.

Figure 7. Changes in fungal and bacterial NO_3^- immobilization rates in relation to their biomass in the surface soil (0 - 20cm). (a) Fungal immobilization rate and fungal PLFA biomass. (b) Bacterial immobilization rate and bacterial PLFA biomass.

Figure 8. Spearman correlations between edaphic factors and microbial PLFA biomass. The color and numbers shown indicate the strength and sign of the correlation. Asterisks denote significance of correlation. $^{*}p < 0.05$, $^{**}p < 0.01$ and $^{***}p < 0.001$. Note: the detailed abbreviation information of environmental factors is shown in Table 1

Fig. 1

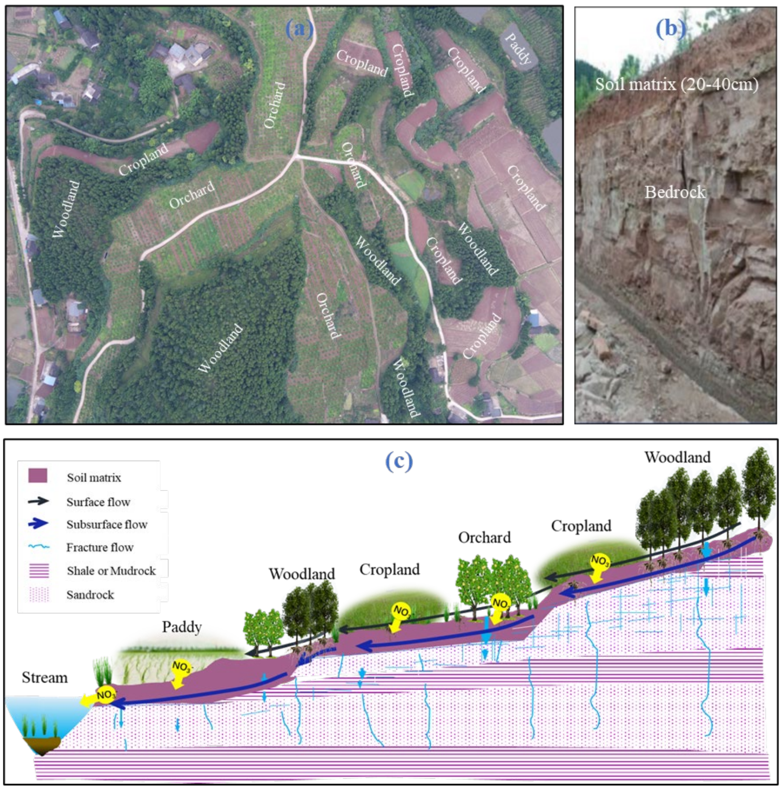
(a)
Cropland
Cropland
Cropland
Paddy
Orchard
Cropland
Orchard
Woodland
Orchard
Cropland
Woodland
Woodland
Cropland
Woodland
Orchard
Cropland
Woodland
Woodland
(b)
Soil matrix (20-40cm)
Bedrock
(c)
Soil matrix
Surface flow
Subsurface flow
Fracture flow
Shale or Mudrock
Sandrock
Woodland
Orchard
Cropland
Woodland
Cropland
Paddy
Stream

Fig. 2

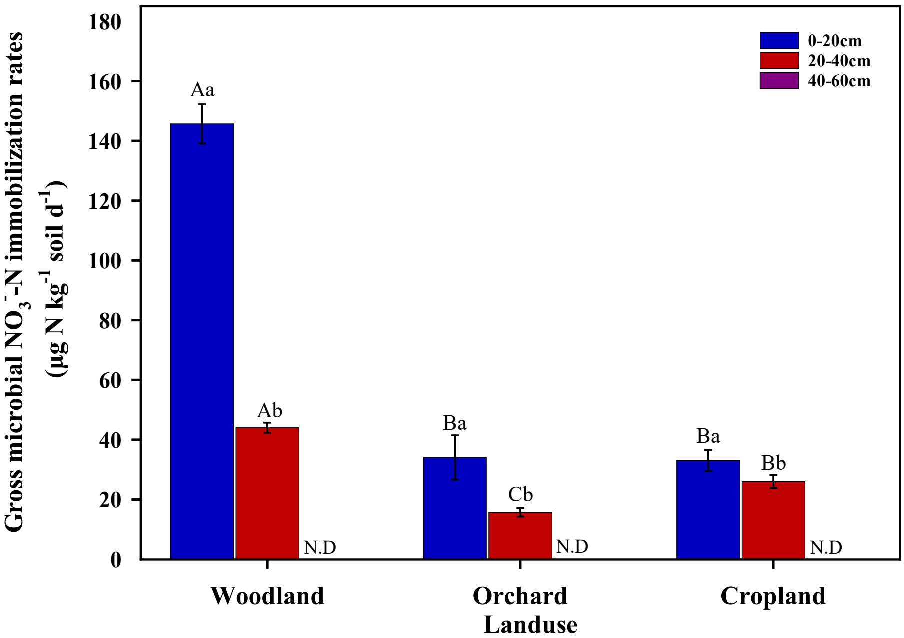

Gross microbial NO_3^--N immobilization rates
($\mu g\ N\ kg^{-1}$ soil d^{-1})
0-20cm
20-40cm
40-60cm
Aa
Ab
N.D
Ba
Cb
N.D
Ba
Bb
N.D
0
20
40
60
80
100
120
140
160
180
Woodland
Orchard
Cropland
Landuse

Fig. 3

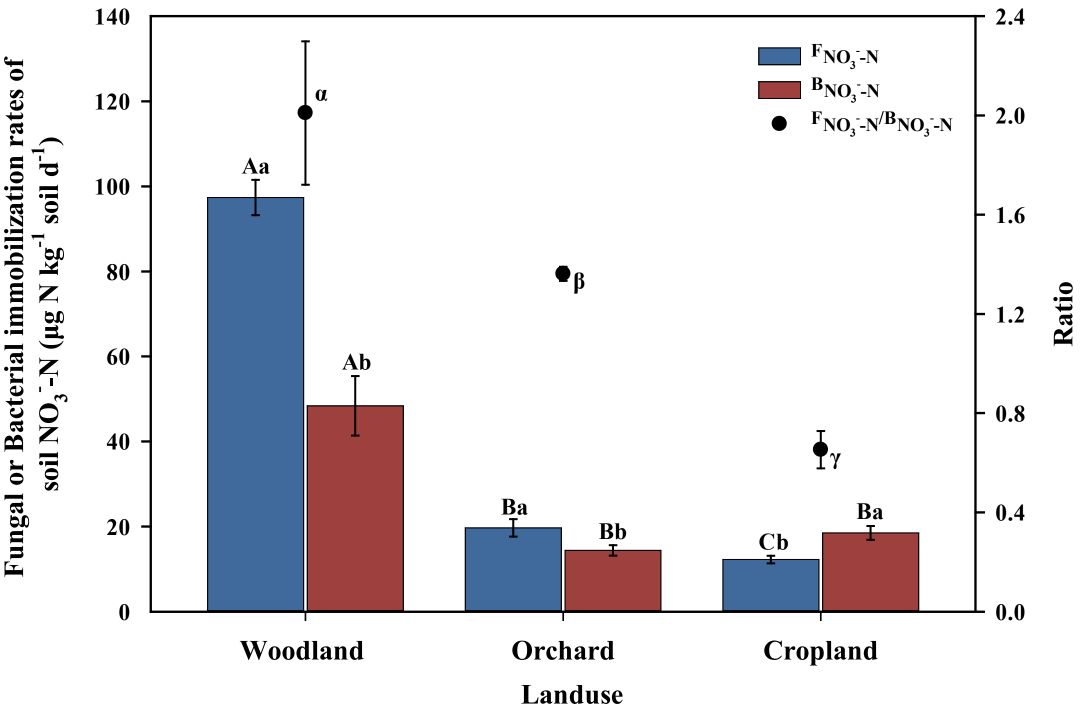
Fungal or Bacterial immobilization rates of soil NO_3^--N (μg N kg^{-1} soil d^{-1})
Ratio
Landuse
Woodland
Orchard
Cropland
$^{F}NO_3^-$-N
$^{B}NO_3^-$-N
$^{F}NO_3^-$-N/$^{B}NO_3^-$-N
Aa
Ab
Ba
Bb
Cb
Ba
α
β
γ
0
20
40
60
80
100
120
140
0.0
0.4
0.8
1.2
1.6
2.0
2.4

Fig. 4

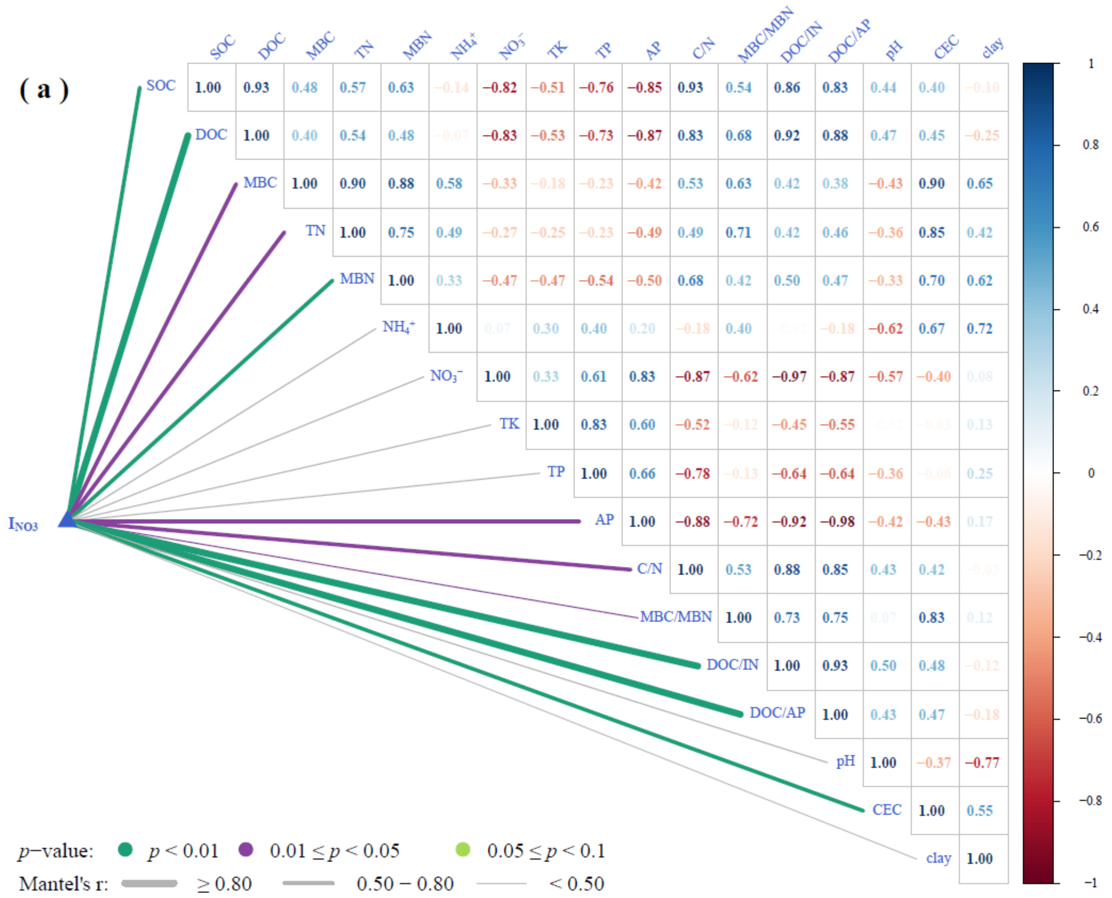

(a)
SOC
DOC
MBC
TN
MBN
NH_4^+
NO_3^-
TK
TP
AP
C/N
MBC/MBN
DOC/IN
DOC/AP
pH
CEC
clay
I_{NO3}
p−value: $p < 0.01$ $0.01 \le p < 0.05$ $0.05 \le p < 0.1$
Mantel's r: ≥ 0.80 $0.50 - 0.80$ < 0.50

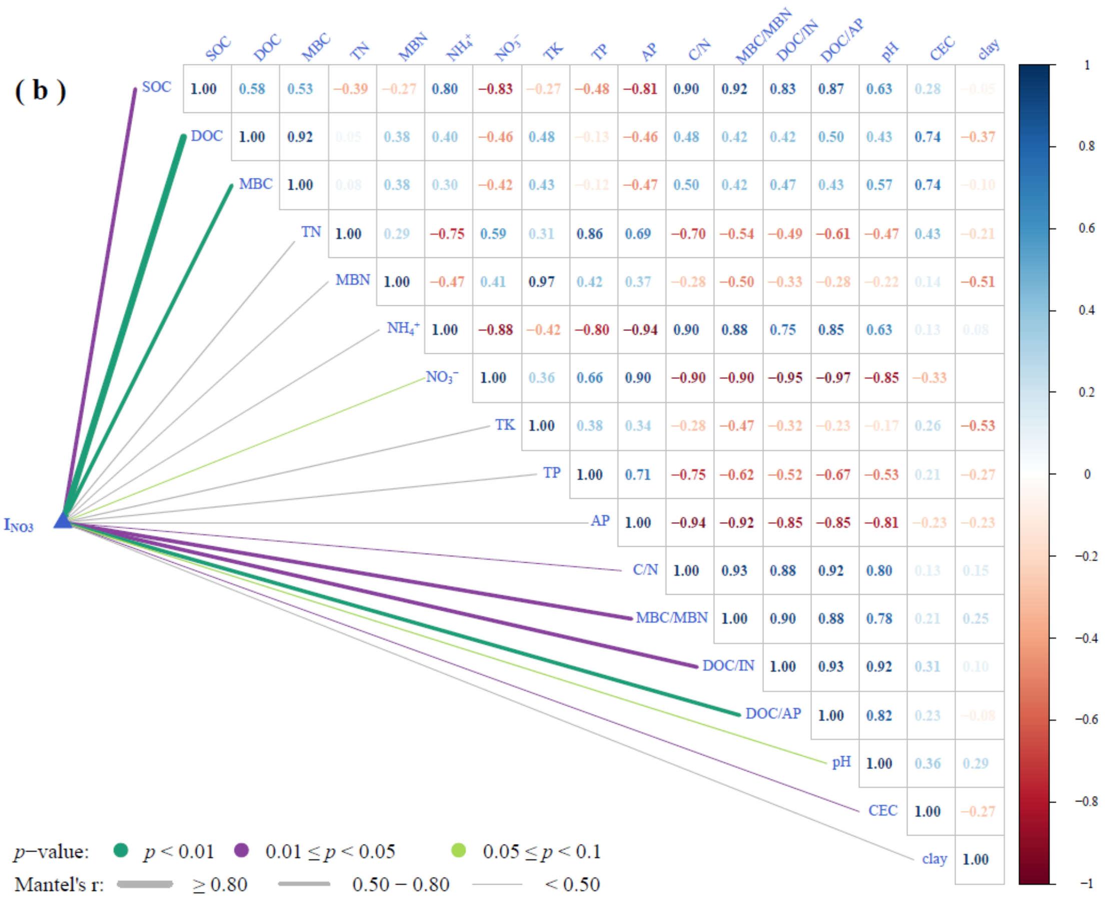

(b)
SOC DOC MBC TN MBN NH4+ NO3− TK TP AP C/N MBC/MBN DOC/IN DOC/AP pH CEC clay
INO3
p−value: p < 0.01 0.01 ≤ p < 0.05 0.05 ≤ p < 0.1
Mantel's r: ≥ 0.80 0.50 − 0.80 < 0.50

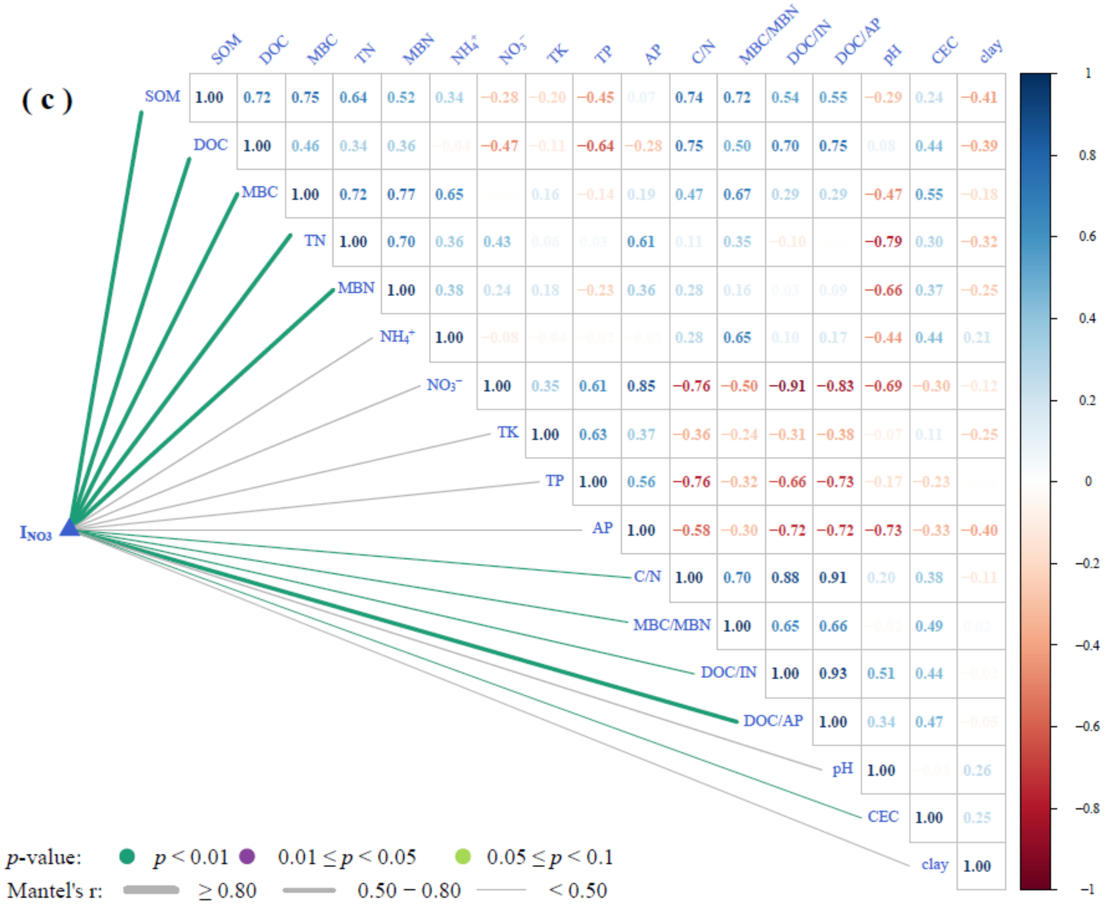

(c)
SOM DOC MBC TN MBN NH4+ NO3− TK TP AP C/N MBC/MBN DOC/IN DOC/AP pH CEC clay
INO3
p-value: p < 0.01 0.01 ≤ p < 0.05 0.05 ≤ p < 0.1
Mantel's r: ≥ 0.80 0.50 − 0.80 < 0.50

Fig. 5

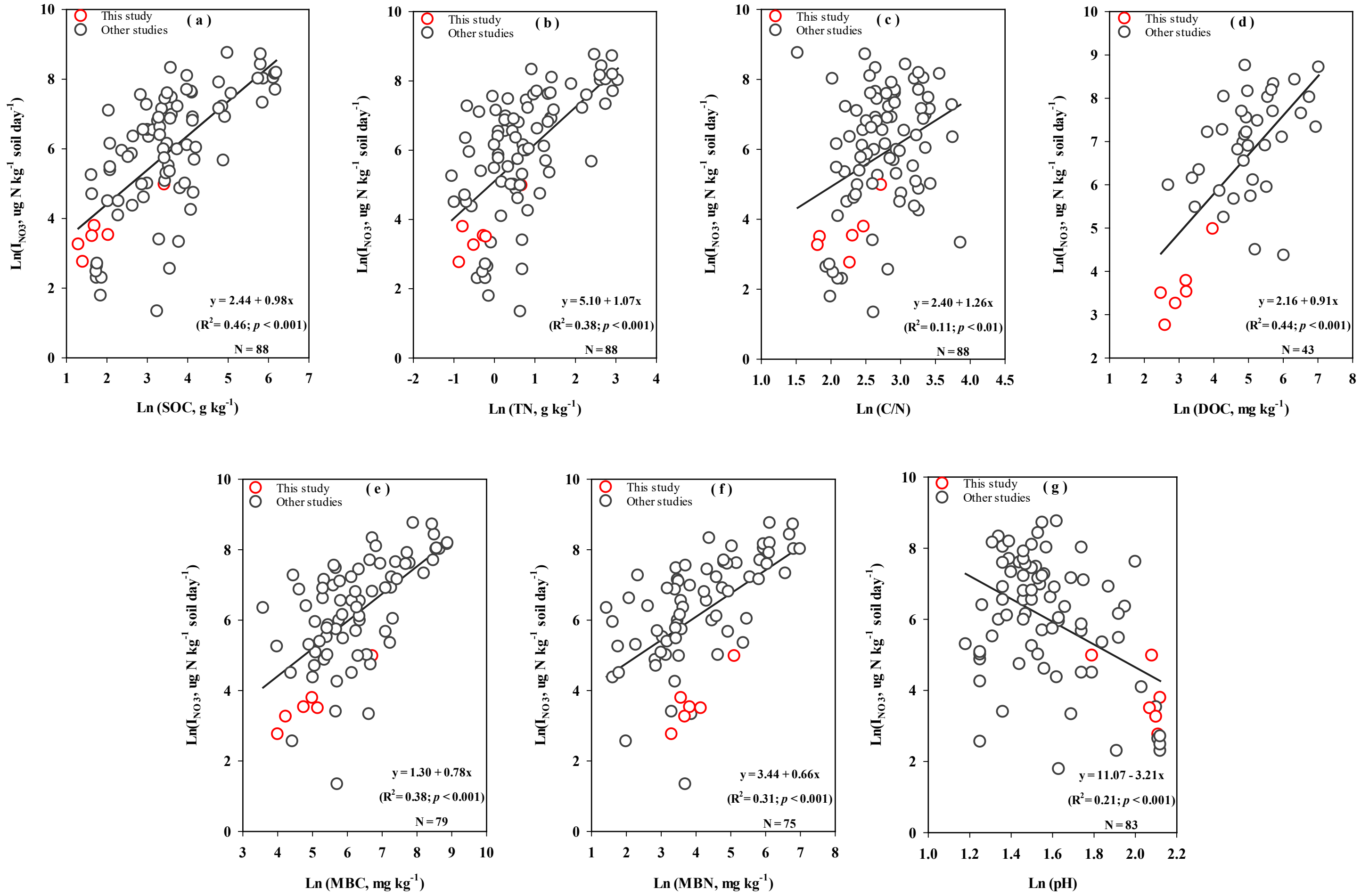
This study
Other studies
(a)
y = 2.44 + 0.98x
(R^2 = 0.46; p < 0.001)
N = 88
Ln (SOC, g kg^{-1})
(b)
y = 5.10 + 1.07x
(R^2 = 0.38; p < 0.001)
N = 88
Ln (TN, g kg^{-1})
(c)
y = 2.40 + 1.26x
(R^2 = 0.11; p < 0.01)
N = 88
Ln (C/N)
(d)
y = 2.16 + 0.91x
(R^2 = 0.44; p < 0.001)
N = 43
Ln (DOC, mg kg^{-1})
(e)
y = 1.30 + 0.78x
(R^2 = 0.38; p < 0.001)
N = 79
Ln (MBC, mg kg^{-1})
(f)
y = 3.44 + 0.66x
(R^2 = 0.31; p < 0.001)
N = 75
Ln (MBN, mg kg^{-1})
(g)
y = 11.07 - 3.21x
(R^2 = 0.21; p < 0.001)
N = 83
Ln (pH)
Ln(I_{NO3}, ug N kg^{-1} soil day^{-1})

Fig. 6

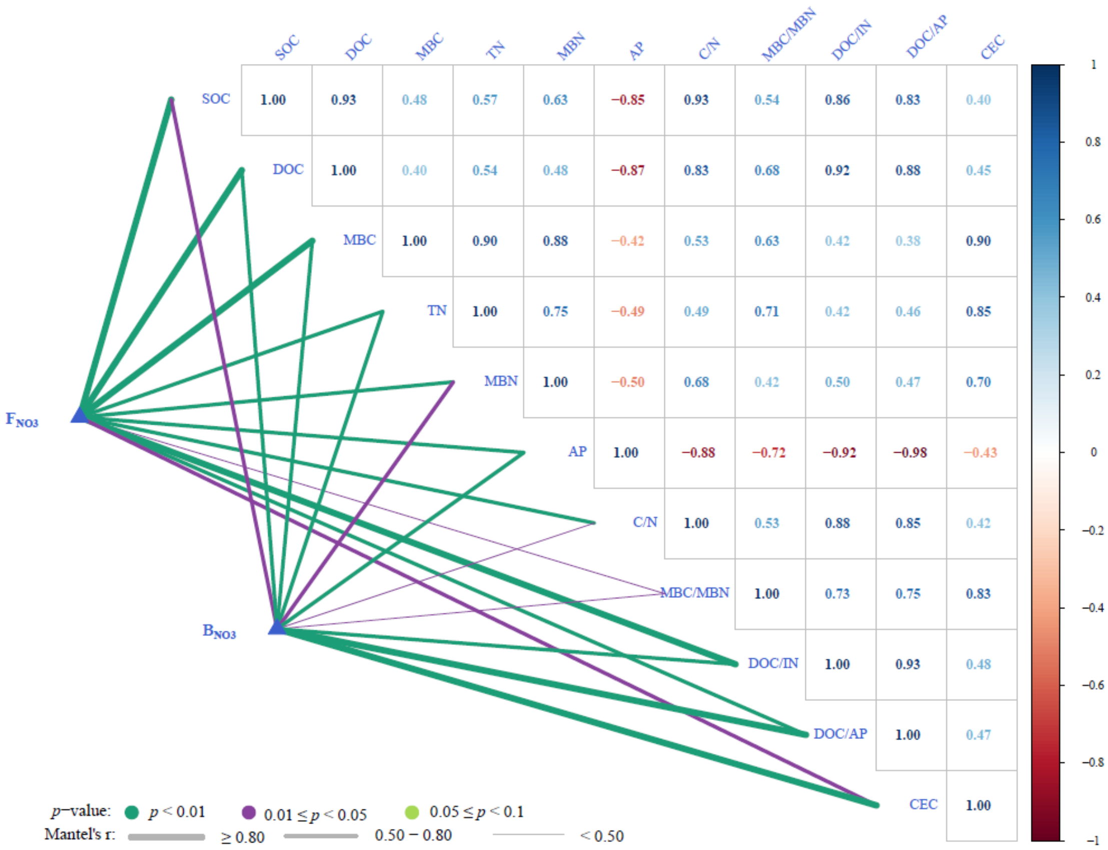
SOC DOC MBC TN MBN AP C/N MBC/MBN DOC/IN DOC/AP CEC
SOC 1.00 0.93 0.48 0.57 0.63 −0.85 0.93 0.54 0.86 0.83 0.40
DOC 1.00 0.40 0.54 0.48 −0.87 0.83 0.68 0.92 0.88 0.45
MBC 1.00 0.90 0.88 −0.42 0.53 0.63 0.42 0.38 0.90
TN 1.00 0.75 −0.49 0.49 0.71 0.42 0.46 0.85
MBN 1.00 −0.50 0.68 0.42 0.50 0.47 0.70
AP 1.00 −0.88 −0.72 −0.92 −0.98 −0.43
C/N 1.00 0.53 0.88 0.85 0.42
MBC/MBN 1.00 0.73 0.75 0.83
DOC/IN 1.00 0.93 0.48
DOC/AP 1.00 0.47
CEC 1.00
F_{NO3}
B_{NO3}
1 0.8 0.6 0.4 0.2 0 −0.2 −0.4 −0.6 −0.8 −1
p−value: p < 0.01 0.01 ≤ p < 0.05 0.05 ≤ p < 0.1
Mantel's r: ≥ 0.80 0.50 − 0.80 < 0.50

Fig. 7

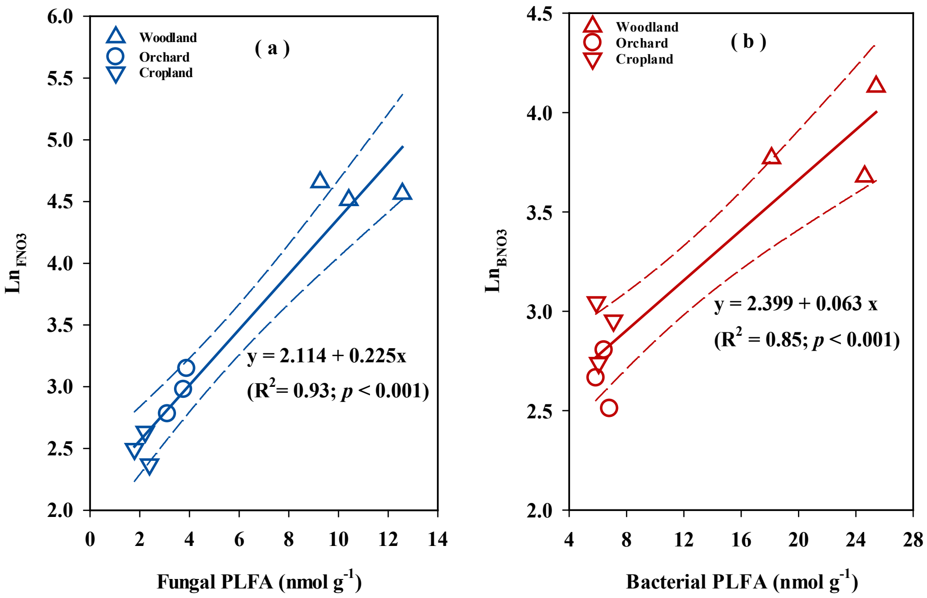
(a)
Woodland
Orchard
Cropland
y = 2.114 + 0.225x
(R^2= 0.93; p < 0.001)
Ln_{FNO3}
Fungal PLFA (nmol g^{-1})
(b)
Woodland
Orchard
Cropland
y = 2.399 + 0.063 x
(R^2 = 0.85; p < 0.001)
Ln_{BNO3}
Bacterial PLFA (nmol g^{-1})

Fig. 8

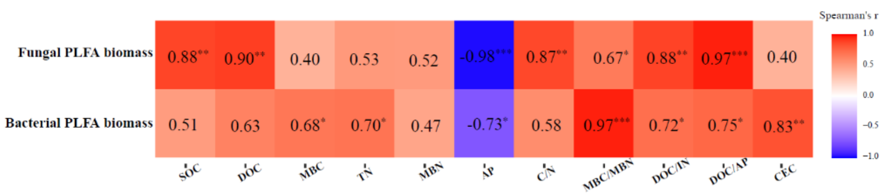
Fungal PLFA biomass
0.88**
0.90**
0.40
0.53
0.52
-0.98***
0.87**
0.67*
0.88**
0.97***
0.40
Bacterial PLFA biomass
0.51
0.63
0.68*
0.70*
0.47
-0.73*
0.58
0.97***
0.72*
0.75*
0.83**
SOC
DOC
MBC
TN
MBN
AP
C/N
MBC/MBN
DOC/TN
DOC/AP
CEC
Spearman's r

Supplementary materials

Land use types affect soil microbial NO_3^- immobilization through changed fungal and bacterial contribution in alkaline soils of a subtropical montane agricultural landscape

Xingling Wang[1,2], Minghua Zhou[1*], Bo Zhu[1], Nicolas Brüggemann[3], Wei Zhang[4], Klaus Butterbach-Bahl[5,6]

[1] Key Laboratory of Mountain Surface Processes and Ecological Regulation, Institute of Mountain Hazards and Environment, Chinese Academy of Sciences, Chengdu 610041, PR China

[2] University of Chinese Academy of Sciences, Beijing 100049, PR China

[3] Institute of Bio- and Geosciences - Agrosphere (IBG-3), Forschungszentrum Jülich GmbH, 52425 Jülich, Germany

[4] Institute of Applied Ecology, Chinese Academy of Sciences, Shenyang 110016, PR China

[5] Pioneer Center Land-CRAFT, Department of Agroecology, Aarhus University, Aarhus C, 8000, Denmark

[6] Institute for Meteorology and Climate Research, Atmospheric Environmental Research, Karlsruhe Institute of Technology, D-82467 Garmisch-Partenkirchen, Germany

Corresponding author: Minghua Zhou E-mail: mhuazhou@imde.ac.cn

Soil microbial community composition analysis

The soil microbial PLFA composition was analyzed in accordance with Frostegård and Bååth (1996). Briefly, lipids were extracted from 8 g of fresh soil with a chloroform-methanol-citrate buffer mixture (1:2:0.8, v/v/v) and separated from nonpolar lipids and derivatized into their corresponding fatty acid methyl esters before analysis. Samples were identified by using an Agilent 6890 N gas chromatography equipped with an identification software (MIDI Inc., Newark, DE, USA). The concentrations of methylated fatty acids were quantified considering with the measurement of methyl nonadecanoate (19:0) as an internal standard. 18:2ω6, 9c was used as the proxy of fungal biomass (Frostegård et al. 2011); i15:0, a15:0, i16:0, 16:1ω9, 16:1ω7c, 10Me16:0, cy17:0, i17:0, a17:0, 18:1ω7 and cy19:0 were used as indicators of bacterial biomass (Frostegård and Bååth 1996).

^{15}N analysis for NO_3^-

The ^{15}N isotopic composition of NO_3^- was determined using the modified micro-diffusion method (Feast and Dennis 1996; Zhang et al. 2011a). In brief, a portion of extract was firstly steam-distilled with MgO to remove all NH_4^+ in the extract for 72h on a mechanical shaker at 140 rpm at 25°C. Subsequently, the extract was distilled again after addition of Devarda's alloy to reduce NO_3^- and the liberated NH_3 was trapped on a Whatman filter (diameter, 0.5 cm) with 10 μL 1M oxalic acid. The ^{15}N enrichment of NO_3^--N and insoluble organic N was measured using an automated C/N analyzer coupled to an isotope ratio mass spectrometer (IRMS 20-22, Sercon, Crewe, UK). Amino-sugar content was analyzed using gas chromatography (Zhang and Amelung

1996). Compound-specific stable isotope analysis of individual amino sugar was performed according to the isotope GC/MS method described by He et al. (2006).

^{15}N analysis for amino sugars

Amino sugars analysis was conducted according to Zhang and Amelung (1996). First, amino sugars were extracted and converted into aldononitrile derivatives. Methyl-glucamine was added as as the recovery standard before derivatization. The derivatives were separated on Agilent 6890A gas chromatograph (GC, Agilent Tech. Co. Ltd., USA) equipped with a HP-5 fused silica column and flame ionization detector. Then, amino sugars were identified and quantified by comparing with the peaks of the standards with respect to the internal standard myo-inositol. The ^{15}N incorporation into GluN and MurN was identified by an isotope GC/MS (Finnigan trace, Thermo Electron Finnigan Co. Ltd., USA) according to He et al. (2006).

Calculation of K_F and K_B

The sum of the estimated fungal NO_3^- immobilization rate and bacterial NO_3^- immobilization rate is equal to the measurable soil gross NO_3^- immobilization rate:

$$I_{NO3} = F_{NO3} + B_{NO3} + e = K_F \times F + K_B \times B + e \qquad (1)$$

where I_{NO3} is the soil gross microbial NO_3^- immobilization rate; F_{NO3} is the fungal NO_3^- immobilization rate; B_{NO3} is the bacterial NO_3^- immobilization rate; K_F is the conversion coefficient from the fungal-derived ^{15}N-GluN synthesis rate to the fungal NO_3^- immobilization rate; K_B is the conversion coefficient from the bacterial-derived ^{15}N-MurN synthesis rate to the bacterial NO_3^- immobilization rate; F is the synthesis rates of fungal-derived ^{15}N-GluN; B is the synthesis rates of bacterial-derived ^{15}N-MurN and

e is the estimation error. Of the variables, I_{NO3}, F and B are obtained experimentally. We used G to replace I_{NO3} and since 3 replicate soil samples were used for the experiment, the equation (1) could be rewritten in a matrix format:

$$\begin{bmatrix} G_1 \\ G_2 \\ G_3 \end{bmatrix} = \begin{bmatrix} F_1 & B_1 \\ F_2 & B_2 \\ F_3 & B_3 \end{bmatrix} \begin{bmatrix} K_F \\ K_B \end{bmatrix} + \begin{bmatrix} e_1 \\ e_2 \\ e_3 \end{bmatrix}$$

If we let $K = \begin{bmatrix} K_F \\ K_B \end{bmatrix}$ and $X = \begin{bmatrix} F_1 & B_1 \\ F_2 & B_2 \\ F_3 & B_3 \end{bmatrix}$, we obtain: $G = X\,K + e$

Alternatively, $e = G - X\,K$.

According to the principle of the least-squares estimators that minimize the sum of the squared residuals, we constructed the 2-Norm of e to find its minimum:

$$E(K) = \left\|e_{(K)}\right\|_2 = \sqrt{\left(\sum_{i=1}^{3} e_i(K)^2\right)} = e^T e$$

$$= (G - X\,K)^T\,(G - X\,K)$$

$$= G^T G - 2K^T X^T G + K^T X^T X\,K$$

Subsequently,

$$\frac{\partial E(K)}{\partial K} = -2\forall(K^T X^T G) + \forall(K^T X^T X\,K) = -2X^T G + 2X^T X\,K = 0$$

Finally, we obtained the K_F and K_B:

$$\hat{K} = (X^T X)^{-1} X^T G$$

The detailed derivation can be found in Wackerly et al. (2014).

Soil fungal and bacterial NO_3^- immobilization intensity

The NO_3^- immobilization intensity of fungi and bacteria were calculated as fungal and bacterial NO_3^- immobilization rates divided by their respective fungal and bacterial biomass with the unit of g N mol^{-1} d^{-1}. Thereby we linked fungal and bacterial NO_3^-

immobilization as a process with the PLFA-derived biomass as a pool to obtain the immobilization quotient for NO_3^- (biomass-specific immobilization).

Supplementary Figures

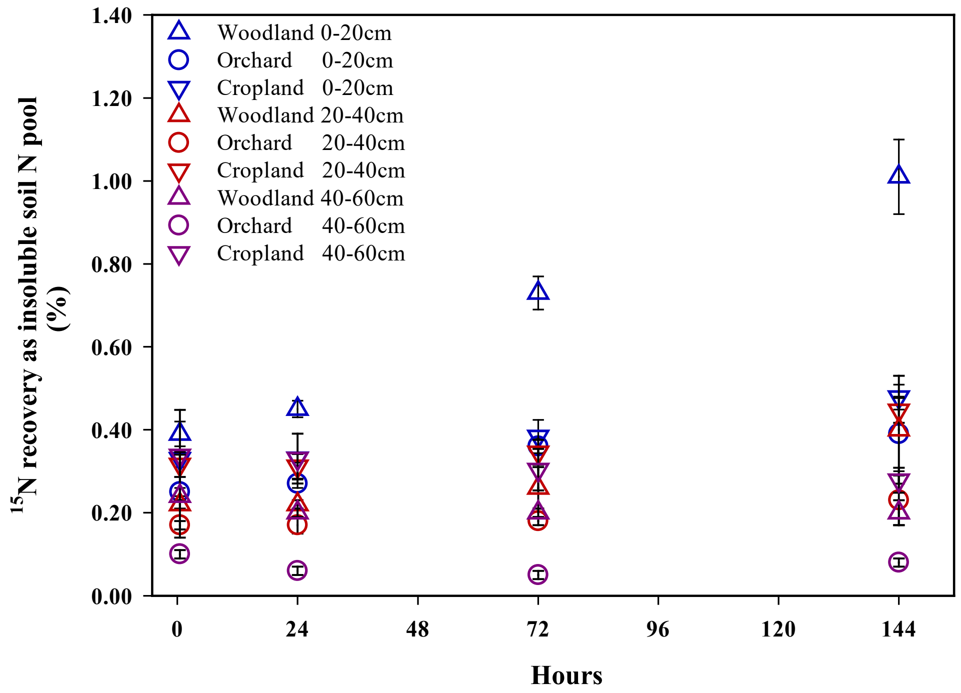

Fig. S1 Percentage of immobilized $^{15}NO_3^-$-N in insoluble organic N pools vs. time under different land use soils.

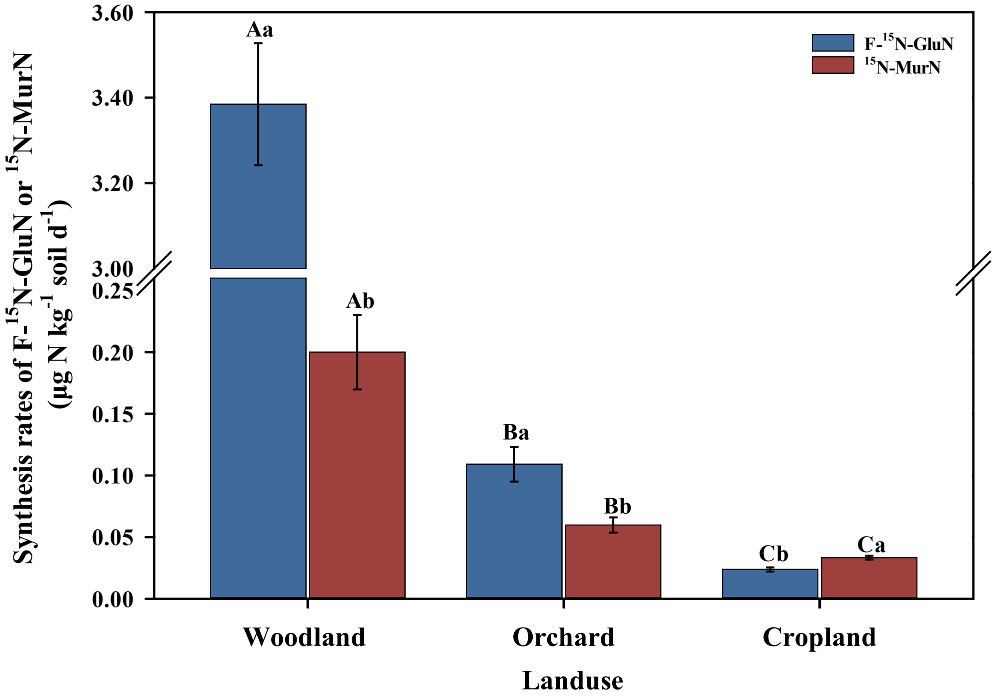

Fig. S2 Synthesis rates of F-^{15}N-GluN and ^{15}N-MurN and under different land use soils in the surface soil (0-20cm). Different letters denote significant differences in the average values among different land use soils at $p < 0.05$. Error bars are standard deviations of the mean (n=3). The invisible error bars are smaller than the symbols.

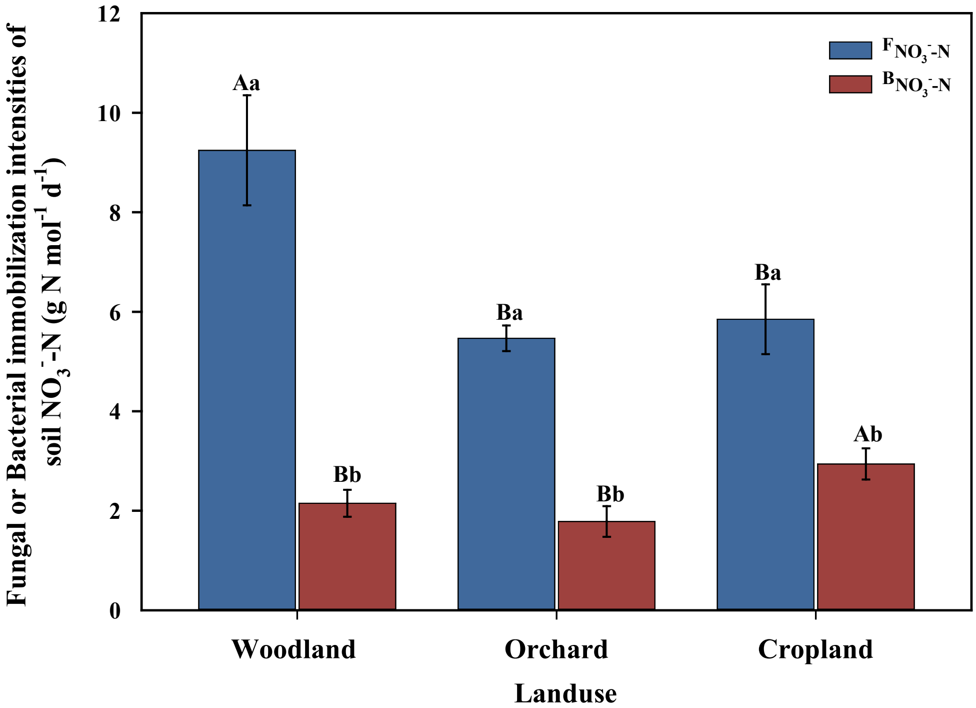

Fig. S3 Fungal and bacterial immobilization intensities of soil NO_3^- under different land uses in the surface soil (0-20 cm). Different letters denote significant differences in the average values among different land use soils at $p < 0.05$. Error bars are standard deviations of the mean (n=3).

Table S1 APE% and concentrations of ammino sugars for top soils

Parameters	GluN ($mg\ kg^{-1}$)	MurN ($mg\ kg^{-1}$)	APE of GluN (%)	APE of MurN (%)
Woodland	895.16 (46.64)	23.75 (6.32)	0.0275 (0.0086)	0.1013 (0.0154)
Orchard	213.16 (21.44)	6.50 (0.26)	0.0117 (0.0009)	0.1157 (0.0114)
Cropland	211.58 (4.96)	7.11 (0.82)	0.0051 (0.0000)	0.0663 (0.0012)

Table S2 Comparisons of studies reporting on soil gross microbial NO_3^- immobilization rates in different regions and for different land uses.

Land use types	Country	Location	Soil depth (cm)	SOC (g kg^{-1})	TN (g kg^{-1})	C/N	DOC (mg kg^{-1})	MBC (mg kg^{-1})	MBN (mg kg^{-1})	pH	Method	I_{NO3} (ug N kg^{-1}soil day^{-1})	Reference
Woodland	Australia	32°38′S, 116°06′E	0-5	20.79	0.49	42.55	35.73	35.70	4.17	5.26	^{15}N pool dilution	570.00	Banning et al. (2008)
	Australia	32°38′S, 116°06′E	0-5	36.75	1.32	28.70	126.85	269.40	45.88	4.66	^{15}N pool dilution	1070.00	Banning et al. (2008)
	Australia	32°38′S, 116°06′E	0-5	28.78	1.04	30.57	133.23	207.25	32.25	4.62	^{15}N pool dilution	1280.00	Banning et al. (2008)
	Australia	32°38′S, 116°06′E	0-5	19.75	0.51	41.95	69.84	85.50	10.24	4.78	^{15}N pool dilution	1440.00	Banning et al. (2008)
	Australia	32°38′S, 116°06′E	0-5	36.66	1.40	29.90	192.66	288.70	30.75	4.57	^{15}N pool dilution	1770.00	Banning et al. (2008)
	Brazil	1°43′3.5″S, 51°27′36″W	0-5	20.10	1.30	15.50	130.00	333.50	35.60	3.90	Microbial biomass ^{15}N recovery	700.00	Sotta et al. (2008)
	Brazil	1°43′3.5″S, 51°27′36″W	0-5	35.80	2.50	14.00	305.00	828.50	80.05	3.80	Microbial biomass ^{15}N recovery	4150.00	Sotta et al. (2008)
	Canada	56°39′N, 111°13′W	0-12	7.54	0.37	9.30	NA	459.00	NA	6.00	^{15}N pool dilution	90.00	Masse et al. (2016)
	Canada	56°39′N, 111°13′W	0-12	136.89	4.00	17.70	NA	1416.00	NA	6.50	^{15}N pool dilution	1010.00	Masse et al. (2016)
	Canada	56.1d°N, 110.9°W	0-15	5.03	0.35	14.37	72.70	53.30	5.80	4.48	^{15}N pool dilution	190.00	Kwak et al. (2018)
	China	31°16′N, 105°28′E	0-20	30.59	1.96	15.14	53.10	826.28	164.84	8.02	Microbial ^{15}N recovery	145.69	This study
	China	31°16′N, 105°28′E	20-40	5.41	0.46	11.77	24.59	147.16	35.58	8.36	Microbial ^{15}N recovery	44.06	This study
	China	23°10′N, 112°10′E	0-20	25.50	1.90	13.60	NA	300.40	40.00	3.90	^{15}N pool dilution	3.80	Han et al. (2018)
	China	23°10′N, 112°10′E	0-20	26.80	2.00	13.50	NA	290.70	27.20	3.88	^{15}N pool dilution	30.00	Han et al. (2018)
	China	24°42′-25°02′N, 107°57′-108°21′E	0-10	60.41	3.79	18.47	NA	2405.80	175.40	7.38	^{15}N pool dilution	2030.00	Li et al. (2018)
	China	41°42′N, 127°38′E	0-15	131.68	10.98	11.99	97.41	1211.71	137.07	5.71	^{15}N pool dilution	290.00	Sun et al. (2016)
	China	27°59′N, 117°25′E	0-20	62.80	3.10	20.30	NA	789.50	NA	4.20	^{15}N pool dilution	114.00	Zhang et al. (2011b)
	China	27°59′N, 117°25′E	0-20	23.20	1.10	21.10	NA	579.00	NA	4.30	^{15}N pool dilution	693.00	Zhang et al. (2011b)
	China		0-20	32.68	2.03	16.09	NA	NA	NA	4.35	^{15}N pool dilution	470.00	Zhang et al. (2013b)

Ecuador	4.115°S; 98.968°W	0-5	61.90	4.10	14.00	240.00	1214.29	116.67	3.90	Microbial biomass ^{15}N recovery	1000.00	Baldos et al. (2015)
Ecuador	4.115°S; 98.968°W	0-5	59.52	4.00	14.00	678.57	1619.05	121.43	4.30	Microbial biomass ^{15}N recovery	2100.00	Baldos et al. (2015)
Germany	51°42′N, 09°40′E	0-5	42.00	2.2	19	14.72	316	32	3.8	Microbial biomass ^{15}N recovery	400.00	Corre et al. (2003)
Germany	49°42′N, 7°18′E	0-5	59.00	2.3	26	NA	302	30	3.5	Microbial biomass ^{15}N recovery	70.00	Corre et al. (2007)
Germany	50°40′N, 13°20′E	0-5	45.00	1.7	26	NA	209	17	3.5	Microbial biomass ^{15}N recovery	130.00	Corre et al. 2007)
Germany	50°24′N, 6°54′E	0-5	51.00	1.6	31	NA	229	23	3.5	Microbial biomass ^{15}N recovery	150.00	Corre et al. (2007)
Germany	49°25′N, 8°42′E	0-5	31.00	1.2	25	NA	163	20	3.5	Microbial biomass ^{15}N recovery	160.00	Corre et al. (2007)
Germany	50°22′N, 12°28′E	0-5	34.00	1.4	24	NA	224	21	3.7	Microbial biomass ^{15}N recovery	250.00	Corre et al. (2007)
Germany	48°25′N, 10°56′W	0-10	32.00	2.00	19.00	NA	134.73	9.66	3.25	^{15}N pool dilution	200.00	Matejek et al. (2010a)
Germany	48°25′N, 10°56′W	0-10	35.00	2.00	16.70	NA	82.69	7.31	3.50	^{15}N pool dilution	13.00	Matejek et al. (2010b)
Indonesia	1°55′40″S;103°15′33″E	0-5	30.00	2.07	13.70	NA	577.70	86.50	4.30	Microbial biomass ^{15}N recovery	400.00	Allen et al. (2015)
Indonesia	1°55′40″S;103°15′33″E	0-5	18.18	1.57	11.70	NA	461.40	73.80	4.50	Microbial biomass ^{15}N recovery	700.00	Allen et al. (2015)
Indonesia	1°55′40″S;103°15′33″E	0-5	26.00	1.83	14.30	NA	514.00	69.70	4.30	Microbial biomass ^{15}N recovery	900.00	Allen et al. (2015)
Indonesia	2°0′57″S;102°45′12″E	0-5	31.11	2.21	14.30	NA	560.70	75.40	4.50	Microbial biomass ^{15}N recovery	1700.00	Allen et al. (2015)

Indonesia	2°0′57″S;102°45′12″E	0-5	33.00	2.63	13.10	NA	1048.10	134.40	4.20	Microbial biomass ^{15}N recovery	2000.00	Allen et al. (2015)
Indonesia	2°0′57″S;102°45′12″E	0-5	53.75	4.14	13.00	NA	922.30	152.80	4.50	Microbial biomass ^{15}N recovery	3300.00	Allen et al. (2015)
Japan	34°57′N 135°59′E	0-10	17.00	0.96	17.60	140.00	275.82	40.40	4.37	^{15}N pool dilution	1900.00	Yokobe et al. (2018)
Japan	34°55′W,135°58′E	0-10	53.40	2.87	18.50	300.00	769.17	121.33	4.32	^{15}N pool dilution	2200.00	Yokobe et al. (2018)
Japan	36°41′N 137°09′E	0-10	53.60	3.43	11.60	168.71	572.40	98.70	3.98	^{15}N pool dilution	450.00	Yokobe et al. (2020)
Japan	36°39′N 137°06′E	0-10	61.80	3.77	12.30	109.22	828.90	138.00	4.49	^{15}N pool dilution	910.00	Yokobe et al. (2020)
Japan	34°55′N 135°58′E	0-10	42.40	2.29	17.00	140.22	453.90	98.70	4.32	^{15}N pool dilution	1360.00	Yokobe et al. (2020)
Japan	35°44′N,139°32′E	0-10	128.00	8.80	9.14	45.64	1440.80	256.60	4.69	^{15}N pool dilution	1360.00	Yokobe et al. (2020)
Japan	43°23′N,144°39′E	0-10	145.40	11.80	4.57	134.71	2664.50	453.90	5.07	^{15}N pool dilution	6360.00	Yokobe et al. (2020)
Japan	36°41′N 137°09′E	organic layer	348.00	15.70	18.60	1041.29	3647.00	714.80	4.04	^{15}N pool dilution	1530.00	Yokobe et al. (2020)
Japan	36°39′N 137°06′E	organic layer	354.50	13.80	24.60	859.18	5179.80	908.00	4.83	^{15}N pool dilution	3050.00	Yokobe et al. (2020)
Japan	43°23′N,144°39′E	organic layer	312.20	21.04	7.55	258.41	5700.95	1081.00	5.69	^{15}N pool dilution	3050.00	Yokobe et al. (2020)
Japan	34°55′N 135°58′E	organic layer	331.70	14.10	21.60	563.30	4925.90	803.00	4.64	^{15}N pool dilution	4580.00	Yokobe et al. (2020)
Japan	35°44′N,139°32′E	organic layer	331.70	18.40	12.10	1121.23	4614.60	888.90	4.70	^{15}N pool dilution	6110.00	Yokobe et al. (2020)
Peru	4.110°S 79.178°W	0-5	454.55	15.64	28.00	72.73	5272.73	381.82	3.90	Microbial biomass ^{15}N recovery	3100.00	Baldos et al. (2015)
Peru	4.110°S 79.178°W	0-5	472.73	13.64	35.00	145.45	7090.91	381.82	3.70	Microbial biomass ^{15}N recovery	3500.00	Baldos et al. (2015)
Portugal	39°20′N, 9°13′W	0-10	13.90	0.57	24.60	410.00	150.00	5.00	5.05	^{15}N pool dilution	79.00	Gomez-Rey et al. (2010)
Portugal	40°30′N,8°18′W	0-10	64.40	3.55	18.20	1920.00	520.00	18.00	4.73	^{15}N pool dilution	297.00	Gómez-Rey et al. (2010)
Portugal	39°19′N, 7°41′W	0-10	10.70	0.54	19.90	250.00	160.00	5.00	5.09	^{15}N pool dilution	382.00	Gómez-Rey et al. (2010)
Portugal	40°13′N 8°00′W	0-10	27.50	2.90	13.20	1720.00	200.00	8.00	4.89	^{15}N pool dilution	750.00	Gómez-Rey et al. (2010)
Portugal	39°21′N 8°53′W	0-10	9.80	0.50	19.80	180.00	80.00	6.00	5.70	^{15}N pool dilution	90.00	Gómez-Rey et al. (2010)
Portugal	38°32′N,8°01′W	0-10	7.70	0.69	10.70	390.00	328.00	33.20	5.73	^{15}N pool dilution	1210.00	Gomez-Rey et al. (2013)

	USA	3.982°S; 79.083°W	0-5	477.78	18.78	26.00	122.22	4777.78	344.44	4.00	Microbial biomass ^{15}N recovery	2200.00	Baldos et al. (2015)
	USA	3.982°S; 79.083°W	0-5	488.89	18.56	26.00	288.89	7222.22	455.56	4.00	Microbial biomass ^{15}N recovery	3600.00	Baldos et al. (2015)
	USA	45°49′N, 77°02′W	0-15	43.80	0.92	47.60	NA	752.00	47.90	5.40	Indirect method	28.00	Hart et al. (1997)
	USA	45°49′N, 77°02′W	0-15	67.00	2.33	28.70	NA	1500.00	235.00	5.10	Indirect method	420.00	Hart et al. (1997)
	USA	45°03′N,120°40′W	0-15	118.00	4.33	27.10	NA	1681.00	332.00	5.40	Indirect method	1290.00	Hart et al. (1997)
	USA	45°03′N,120°40′W	0-15	160.00	9.74	16.40	NA	2172.00	419.00	3.90	Indirect method	1980.00	Hart et al. (1997)
	USA	45°03′N,120°40′W	0-15	118.00	6.70	17.60	NA	2264.00	444.00	4.30	Indirect method	2720.00	Hart et al. (1997)
	USA	42°22′N˜ 85°30′W	0-10	20.00	1.50	13.40	NA	708.33	102.50	4.60	Microbial biomass ^{15}N recovery	150.00	Holmes and Zak (1999)
	USA	42°22′N˜ 85°30′W	0-10	35.00	3.90	9.00	NA	1382.00	212.50	6.30	Microbial biomass ^{15}N recovery	210.00	Holmes and Zak (1999)
	USA	44°N,84°W	0-10	27.50	1.09	25.37	NA	124.30	13.70	3.53	^{15}N pool dilution	600.00	LeDuc and Rothstein(2007)
	USA	41°45′N˜ 11°48′W	0-10	35.50	1.30	27.80	NA	102.00	30.00	NA	^{15}N pool dilution	960.00	Chen and Stark(2000)
	Australia	31°28′S˜ 118°16′E	0-5	13.63	1.10	12.39	64.55	233.30	31.70	5.67	^{15}N pool dilution	350.00	Hoyle and Murphy(2006)
Agricultural land	China	31°16′N, 105°28′E	0-20	7.62	0.76	10.08	24.90	115.78	45.65	8.16	Microbial ^{15}N recovery	34.10	This study
	China	31°16′N, 105°28′E	20-40	4.06	0.42	9.68	13.43	54.75	27.21	8.25	Microbial ^{15}N recovery	15.75	This study
	China	31°16′N, 105°28′E	0-20	5.10	0.81	6.30	11.93	173.16	63.07	7.91	Microbial ^{15}N recovery	33.10	This study
	China	31°16′N, 105°28′E	20-40	3.64	0.60	6.11	18.16	68.82	39.70	8.17	Microbial ^{15}N recovery	26.03	This study
	China	24°42′-25°02′N˜ 107°57′-108°21′E	0-10	17.56	1.90	10.76	NA	549.08	33.36	5.99	^{15}N pool dilution	145.00	Li et al. (2018)
	China	24°42′-25°02′N˜ 107°57′-108°21′E	0-10	14.14	1.70	9.68	NA	529.42	37.72	7.03	^{15}N pool dilution	580.00	Li et al. (2018)
	China	31°16′N, 105°28′E	0-20	6.32	0.87	7.29	NA	NA	NA	5.09	^{15}N pool dilution	6	Zhang et al. (2022)
	China	31°16′N, 105°28′E	0-20	5.70	0.66	8.69	NA	NA	NA	6.75	^{15}N pool dilution	10	Zhang et al. (2022)
	China	31°16′N, 105°28′E	0-20	9.74	1.19	8.17	NA	NA	NA	7.65	^{15}N pool dilution	60	Zhang et al. (2022)
	China	31°16′N, 105°28′E	0-20	5.75	0.84	6.87	NA	NA	NA	8.22	^{15}N pool dilution	14	Zhang et al. (2022)

China	31°16′N, 105°28′E	0-20	6.47	0.8	8.13	NA	NA	NA	8.37	^{15}N pool dilution	10	Zhang et al. (2022)
China	31°16′N, 105°28′E	0-20	5.65	0.75	7.65	NA	NA	NA	8.37	^{15}N pool dilution	12	Zhang et al. (2022)
China	31°16′N, 105°28′E	0-20	5.80	0.8	7.25	NA	NA	NA	8.37	^{15}N pool dilution	15.00+	Zhang et al. (2022)
China		0-20	18.35	1.78	10.32	NA	NA	NA	4.77	^{15}N pool dilution	100.00	Zhang et al. (2013b)
Spain	39°19′N, 05°19′W	0-10	30.60	1.78	17.24	158.57	292.50	36.35	4.96	^{15}N pool dilution	310.00	Vázquez et al. (2019)
Spain	39°19′N, 05°19′W	0-10	26.70	1.61	16.58	147.28	199.70	24.16	5.00	^{15}N pool dilution	990.00	Vázquez et al. (2019)
USA	32°04′N,82°07′W	0-10	5.10	0.48	10.63	NA	157.00	17.30	NA	^{15}N pool dilution	110.00	Muruganandam et al. (2010)
USA	32°04′N,82°07′W	0-10	8.00	0.72	11.11	NA	183.00	23.80	NA	^{15}N pool dilution	220.00	Muruganandam et al. (2010)
USA	32°04′N,82°07′W	0-10	12.50	1.10	11.36	NA	225.00	30.50	NA	^{15}N pool dilution	320.00	Muruganandam et al. (2010)
USA	38°32′N, 121°52′W	0-8	8.00	1.00	8.00	31.95	357.30	31.00	6.80	Microbial ^{15}N recovery	240.00	Bowles et al. (2015)
USA	38°32′N, 121°52′W	0-8	8.00	1.00	8.00	29.45	351.60	34.50	6.80	Microbial ^{15}N recovery	470.00	Bowles et al. (2015)

I_{NO3}, the gross microbial NO_3^- immobilization rate

References

Allen K, Corre MD, Tjoa A, Veldkamp E (2015) Soil Nitrogen-Cycling Responses to Conversion of Lowland Forests to Oil Palm and Rubber Plantations in Sumatra, Indonesia. PLoS One 10:e0133325

Baldos AP, Corre MD, Veldkamp E (2015) Response of N cycling to nutrient inputs in forest soils across a 1000-3000 m elevation gradient in the Ecuadorian Andes. Ecology 96:749-761

Banning NC, Grant CD, Jones DL, Murphy DV (2008) Recovery of soil organic matter, organic matter turnover and nitrogen cycling in a post-mining forest rehabilitation chronosequence. Soil Biol Biochem 40:2021-2031

Bowles TM, Raab PA, Jackson LE (2015) Root expression of nitrogen metabolism genes reflects soil nitrogen cycling in an organic agroecosystem. Plant Soil 392:175-189

Chen J, Stark JM (2000) Plant species effects and carbon and nitrogen cycling in a sagebrush-crested wheatgrass soil. Soil Biol Biochem 32:47-57

Corre MD, Beese FO, Brumme R (2003) Soil nitrogen cycle in high nitrogen deposition forest: Changes under nitrogen saturation and liming. Ecol Appl 13:287-298

Corre MD, Brumme R, Veldkamp E, Beese FO (2007) Changes in nitrogen cycling and retention processes in soils under spruce forests along a nitrogen enrichment gradient in Germany. Global Change Biol 13:1509-1527

Feast NA, Dennis PF (1996) A comparison of methods for nitrogen isotope analysis of groundwater. Che Geol 129:167-171

Frostegård A, Bååth E (1996) The use of phospholipid fatty acid analysis to estimate bacterial and fungal biomass in soil. Biol Fertil Soils 22:59-65

Frostegård A, Tunlid A, Bååth E (2011) Use and misuse of PLFA measurements in soils. Soil Biol Biochem 43:1621-1625

Gomez-Rey MX, Madeira M, Gonzalez-Prieto SJ, Coutinho J (2010) Soil C and N dynamics within a precipitation gradient in Mediterranean eucalypt plantations. Plant Soil 336:157-171

Gomez-Rey MX, Madeir M, Jesus Gonzalez-Prieto, S, Coutinho J (2013) Soil C and N dynamics in a Mediterranean oak woodland with shrub encroachment. Plant Soil 371:339-354

Han XG, Shen WJ, Zhang JB, Müller C (2018) Microbial adaptation to long-term N supply prevents large responses in N dynamics and N losses of a subtropical forest. Sci Total Environ 626:1175-1187

Hart SC, Binkley D, Perry DA (1997) Influence of red alder on soil nitrogen transformations in two conifer forests of contrasting productivity. Soil Biol Biochem 29:1111-1123

He HB, Xie HT, Zhang XD (2006) A novel GC/MS technique to assess ^{15}N and ^{13}C incorporation into soil amino sugars. Soil Biol Biochem 38:1083-1091

Holmes WE, Zak DR (1999) Soil microbial control of nitrogen loss following clearcut harvest in northern hardwood ecosystems. Ecol Appl 9:202-215

Hoyle FC, Murphy DV (2006) Seasonal changes in microbial function and diversity associated with stubble retention versus burning. Aust J Soil Res 44:407-423

Kwak JH, Naeth MA, Chang SX (2018) Microbial Activities and Gross Nitrogen Transformation Unaffected by Ten-Year Nitrogen and Sulfur Addition. SSSAJ 82:362-370

LeDuc SD, Rothstein DE (2007) Initial recovery of soil carbon and nitrogen pools and dynamics following disturbance in jack pine forests: A comparison of wildfire and clearcut harvesting. Soil Biol Biochem 39:2865-2876

Li DJ, Liu J, Chen H, Zheng L, Wan KL (2018) Soil gross nitrogen transformations in responses to land use conversion in a subtropical karst region. J Environ Manage 212:1-7

Masse J, Prescott CE, Müller C, Grayston SJ (2016) Gross nitrogen transformation rates differ in reconstructed oil-sand soils from natural boreal-forest soils as revealed using a ^{15}N tracing method. Geoderma 282:37-48

Matejek B, Huber C, Dannenmann M, Kohlpaintner M, Gasche R, Göttlein A, Papen H (2010a) Microbial nitrogen-turnover processes within the soil profile of a nitrogen-saturated spruce forest and their relation to the small-scale pattern of seepage-water nitrate. J Plant Nutr Soil Sc 173:224-236

Matejek B, Huber C, Dannenmann M, Kohlpaintner M, Gasche R, Papen H (2010b) Microbial N turnover processes in three forest soil layers following clear cutting of an N saturated mature spruce stand. Plant Soil 337:93-110

Muruganandam S, Israel DW, Robarge WP (2010) Nitrogen Transformations and Microbial Communities in Soil Aggregates from Three Tillage Systems. SSSAJ 74:120-129

Sotta ED, Corre MD, Veldkamp E (2008) Differing N status and N retention processes of soils under old-growth lowland forest in Eastern Amazonia, Caxiuana, Brazil. Soil Biol Biochem 40:740-750

Sun JF, Peng B, Li W, Qu GF, Dai WW, Dai GH, Jiang P, Han SJ, Bai E (2016) Effects of Nitrogen Addition on Potential Soil Nitrogen-Cycling Processes in a Temperate Forest Ecosystem. Soil Sci 181:29-38

Vázquez E, Benito M, Navas M, Espejo R, Díaz-Pinés E, Teutscherova N (2019) The interactive effect of no-tillage and liming on gross N transformation rates during the summer fallow in an acid Mediterranean soil. Soil Tillage Res 194: 104297

Wackerly D, Mendenhall W, Scheaffer RL (2014) Mathematical Statistics with Applications. Cengage Learning

Yokobe T, Hyodo FJ, Tokuchi N (2018) Seasonal Effects on Microbial Community Structure and Nitrogen Dynamics in Temperate Forest Soil. Forests 9:153

Yokobe T, Hyodo FJ, Tokuchi N (2020) Volcanic deposits affect soil nitrogen dynamics and fungal-bacterial dominance in temperate forests. Soil Biol Biochem 150:108011

Zhang XD, Amelung W (1996) Gas chromatographic determination of muramic acid, glucosamine, mannosamine, and galactosamine in soils. Soil Biol Biochem 28:1201-1206

Zhang JB, Zhu TB, Cai ZC, Müller C (2011a) Nitrogen cycling in forest soils across climate gradients in Eastern China. Plant Soil 342:419-432

Zhang JB, Müller C, Zhu TB, Cheng Y, Cai ZC (2011b) Heterotrophic nitrification is the predominant NO_3^- production mechanism in coniferous but not broad-leaf acid forest soil in subtropical China. Biol Fert Soils 47:533-542